

Cosmic-ray propagation and interactions in the Galaxy

ANDREW W. STRONG¹, IGOR V. MOSKALENKO², VLADIMIR S. PTUSKIN³

1. Max-Planck-Institut für extraterrestrische Physik, Postfach 1312, 85741 Garching, Germany. *aws@mpe.mpg.de*

2. Hansen Experimental Physics Laboratory (HEPL) and KIPAC, Stanford University, Stanford, CA 94305, U.S.A. *imos@stanford.edu*

3. Institute for Terrestrial Magnetism, Ionosphere and Radiowave Propagation of the Russian Academy of Sciences (IZMIRAN), Troitsk, Moscow region 142190, Russia. *vptuskin@izmiran.ru*

Key Words energetic particles, gamma rays, interstellar medium, magnetic fields, plasmas *This draft was made on November 26, 2024.*

Abstract

We survey the theory and experimental tests for the propagation of cosmic rays in the Galaxy up to energies of 10^{15} eV. A guide to the previous reviews and essential literature is given, followed by an exposition of basic principles. The basic ideas of cosmic-ray propagation are described, and the physical origin of its processes are explained. The various techniques for computing the observational consequences of the theory are described and contrasted. These include analytical and numerical techniques. We present the comparison of models with data including direct and indirect – especially gamma-ray – observations, and indicate what we can learn about cosmic-ray propagation. Some particular important topics including electrons and antiparticles are chosen for discussion.

CONTENTS

Introduction	2
Cosmic-ray Propagation: Theory	3
<i>Basics and Approaches</i>	3
<i>Propagation equation</i>	4
<i>Diffusion</i>	5
<i>Convection</i>	6
<i>Reacceleration</i>	7
<i>Galactic structure</i>	8
<i>Interactions</i>	9
<i>Weighted Slabs and Leaky Boxes</i>	9
<i>Explicit models</i>	11
<i>GALPROP</i>	11
<i>Numerical versus analytical</i>	13
<i>Self-consistent models</i>	13

Confrontation of Theory with Data	14
<i>Stable secondary/primary ratios</i>	14
<i>Unstable secondary/primary ratios: ‘radioactive clocks’</i>	15
<i>K-capture isotopes and acceleration delay</i>	16
<i>K-capture isotopes and reacceleration</i>	16
<i>Anisotropy</i>	17
<i>Diffuse Galactic Gamma Rays</i>	18
<i>Antiprotons and positrons</i>	20
<i>Electrons and Synchrotron Radiation</i>	22
<i>Time- and space-dependent effects</i>	23
Summary Points list	23
Future Issues	24
Related Resources	24
Key terms, definitions and acronyms	24
Acknowledgements	24

1 Introduction

Cosmic rays (hereafter CR) are almost unique in astrophysics in that they can be directly sampled, not just observed via electromagnetic radiation. Other examples are meteorites and stardust. CR provide us with a detailed elemental and isotopic sample of the current (few million years old) interstellar medium not available in any other way. It is this which makes the subject especially rich and complementary to other disciplines.

CR have featured frequently in Annual Reviews: about 15 articles from 1952 to 1989! Reviews include heavy nuclei (1), collective transport effects (2), composition (3) and propagation (4). Cox’s recent Annual Review ‘The Three Phase Interstellar Medium’ (5) contains much discussion of CR as one essential component of the interstellar medium (ISM), but inevitably no mention of their propagation. Two recent AnnRev articles (6; 7) give extensive discussion of the relation of CR to turbulence which means we do not try to cover this also.

A basic reference is the book ‘Astrophysics of Cosmic Rays’ (8) which expounds all the essential concepts, and is an update of the classic ‘The Origin of Cosmic Rays’ (9) which laid the modern foundations of the subject, with an updated presentation in (10). Good books for basic expositions are (11; 12) and for high energies (13). A basic text emphasizing theory is (14), while the book ‘Astrophysics of Galactic Cosmic Rays’ (15) gives an valuable overview of the experimental data and theoretical ideas as of 2001. The bi-annual International Cosmic Ray Conference proceedings¹ are also an essential source of information, especially for the latest news on the subject.

Recently a plethora of reviews have appeared on the subject of CR above 10^{15} eV, e.g. (16; 17; 18); on interactions (19), on experiments and astrophysics (20), more on astrophysics, propagation and composition (21; 22; 23), and a review of models (24); we recommend (25) and the very up to date (26; 27). Therefore this topic has been excluded here. At the lowest energy end, we note that MeV particles are non-thermal (even if not relativistic) and must be mentioned in a

¹the recent conferences are available via the NASA Astrophysics Data System ADS

review of CR, especially since they are important sources of heating and ionization of the interstellar medium (28). As one example of their far-ranging influence, star formation in molecular clouds may be suppressed by CR produced in SNR nearby (29).

It is worth distinguishing between two ways of approaching CR propagation: either from the *particle* point-of-view, including the spectrum and interactions, or treating the CR as a weightless collisionless relativistic *gas* with pressure and energy and considering it alongside other components of the interstellar medium (30; 31). Both ways of looking at the problem are valid up to a point, but for consistency a unified approach would be desirable and to our knowledge has never been attempted. The nearest approach to this is (32; 33). Most papers address exclusively one or the other aspect. The first approach is required for comparison with observations of CR (direct and indirect) while the second is required for the ISM: stability, heating etc. (5).

The major recent advances in the field are the high quality measurements of isotopic composition and element spectra, and observations by gamma-ray telescopes, both satellite and ground-based. Space does not allow any discussion of the observational data here, but the figures give an illustrative overview of what is now available from both direct (Figs. 1–13) and indirect (γ -ray) measurements (Figs. 14, 16). Concerning the *origin* of CR, we follow Cesarsky’s 1980 Annual Review (4) ‘we will, for the most part, sidestep this problem.’ Hence we omit CR sources including composition and acceleration; for supernova remnants as CR sources the literature can be traced back from the most recent H.E.S.S. TeV γ -ray results (34). We also omit solar modulation, galaxy clusters and extragalactic CR. We mostly restrict attention to our own Galaxy, but mention important information coming from external galaxies (via synchrotron radiation).

We first introduce the theoretical background, and then consider the confrontation of theory with observation. A number of particular topics are selected for further discussion.

2 Cosmic-ray Propagation: Theory

2.1 Basics and Approaches

We present the basic concepts of CR propagation, and techniques for relating these to observational data. Practically all our knowledge of CR propagation comes via secondary CR, with additional information from γ -rays and synchrotron radiation. It is useful at the outset to point out why secondary nuclei in particular are a good probe of CR propagation: the fact that the primary nuclei are measured (at least locally) means that the secondary production functions can be computed from primary spectra, cross-sections and interstellar gas densities with reasonable precision; the secondaries can then be ‘propagated’ and compared with observations.

Since the realization that CR fill the Galaxy it has been clear that nuclear interactions imply that their composition contains information on their propagation (44). A historical event was the arrival of satellite measurements of isotopic Li, Be, B in the 1970’s (45). Since then the subject has expanded enormously with models of increasing degrees of sophistication. The simple observation that the observed composition of CR is different from that of solar, in that rare solar-system nuclei like Boron are abundant in CR, proves the importance of propaga-

tion in the interstellar medium. The canonical ‘few g cm⁻²’ of traversed material is one of the widest-known facts of cosmic-ray physics.

At present we believe that the diffusion model with possible inclusion of convection provides the most adequate description of CR transport in the Galaxy at energies below about 10¹⁷ eV so we begin by presenting this model.

2.2 Propagation equation

The CR propagation equation for a particular particle species can be written in the general form:

$$\begin{aligned} \frac{\partial \psi(\vec{r}, p, t)}{\partial t} &= q(\vec{r}, p, t) + \vec{\nabla} \cdot (D_{xx} \vec{\nabla} \psi - \vec{V} \psi) \\ &+ \frac{\partial}{\partial p} p^2 D_{pp} \frac{\partial}{\partial p} \frac{1}{p^2} \psi - \frac{\partial}{\partial p} \left[\dot{p} \psi - \frac{p}{3} (\vec{\nabla} \cdot \vec{V}) \psi \right] - \frac{1}{\tau_f} \psi - \frac{1}{\tau_r} \psi \quad (1) \end{aligned}$$

where $\psi(\vec{r}, p, t)$ is the CR density per unit of total particle momentum p at position \vec{r} , $\psi(p)dp = 4\pi p^2 f(\vec{p})dp$ in terms of phase-space density $f(\vec{p})$, $q(\vec{r}, p)$ is the source term including primary, spallation and decay contributions, D_{xx} is the spatial diffusion coefficient, \vec{V} is the convection velocity, diffusive reacceleration is described as diffusion in momentum space and is determined by the coefficient D_{pp} , $\dot{p} \equiv dp/dt$ is the momentum gain or loss rate, τ_f is the time scale for loss by fragmentation, and τ_r is the time scale for radioactive decay.

CR sources are usually assumed to be concentrated near the Galactic disk and to have a radial distribution like for example supernova remnants (SNR). A source injection spectrum and its isotopic composition are required; composition is usually initially based on primordial solar but can be determined iteratively from the CR data themselves for later comparison with solar. The spallation part of $q(\vec{r}, p, t)$ depends on all progenitor species and their energy-dependent cross-sections, and the gas density $n(\vec{r})$; it is generally assumed that the spallation products have the same kinetic energy per nucleon as the progenitor. K-electron capture and electron stripping can be included via τ_f and q . D_{xx} is in general a function of $(\vec{r}, \beta, p/Z)$ where $\beta = v/c$ and Z is the charge, and p/Z determines the gyroradius in a given magnetic field; D_{xx} may be isotropic, or more realistically anisotropic, and may be influenced by the CR themselves (e.g. in wave-damping models). D_{pp} is related to D_{xx} by $D_{pp} D_{xx} \propto p^2$, with the proportionality constant depending on the theory of stochastic reacceleration (8; 46) as described in Section 2.5. \vec{V} is a function of \vec{r} and depends on the nature of the Galactic wind. The term in $\vec{\nabla} \cdot \vec{V}$ represents adiabatic momentum gain or loss in the non-uniform flow of gas with a frozen-in magnetic field whose inhomogeneities scatter the CR. τ_f depends on the total spallation cross-section and $n(\vec{r})$. $n(\vec{r})$ can be based on surveys of atomic and molecular gas, but can also incorporate small-scale variations such as the region of low gas density surrounding the Sun. The presence of interstellar helium at about 10% of hydrogen by number must be included; heavier components of the ISM are not important for producing CR by spallation. This equation only treats continuous momentum-loss; catastrophic losses can be included via τ_f and q . CR electrons, positrons and antiprotons propagation constitute just special cases of this equation, differing only in their energy losses and production rates.

The *boundary conditions* depend on the model; often $\psi = 0$ is assumed at the ‘halo boundary’ where particles escape into intergalactic space, but this obviously

just an approximation (since the intergalactic flux is not zero) which can be relaxed for models with a physical treatment of the boundary.

Equation (1) is a time-dependent equation; usually the steady-state solution is required, which can be obtained either by setting $\partial\psi/\partial t = 0$ or following the time dependence until a steady state is reached; the latter procedure is much easier to implement numerically. The time-dependence of q is neglected unless effects of nearby recent sources or the stochastic nature of sources are being studied. Starting with the solution for the heaviest primaries and using this to compute the spallation source for their products, the complete system can be solved including secondaries, tertiaries etc. Then the CR spectra at the solar position can be compared with direct observations, including solar modulation if required.

Source abundances are determined iteratively, comparing propagation calculations with data; for nuclei with very small source abundances, the source values are masked by secondaries and cross-section uncertainties and are therefore hard to determine. Webber (47) gives a ranking from ‘easy’ to ‘impossible’ for the possibility of getting the source abundances using ACE data. A recent review of the high-precision abundances from ACE is in (48) and for Ulysses in (49). For a useful summary of the various astrophysical abundances relevant to interpreting CR abundances see (50).

2.3 Diffusion

The concept of CR diffusion explains why energetic charged particles have highly isotropic distributions and why they are retained well in the Galaxy. The Galactic magnetic field which tangles the trajectories of particles plays a crucial role in this process. Typical values of the diffusion coefficient found from fitting to CR data is $D_{xx} \sim (3 - 5) \times 10^{28} \text{ cm}^2 \text{ s}^{-1}$ at energy $\sim 1 \text{ GeV/n}$ and it increases with magnetic rigidity as $R^{0.3} - R^{0.6}$ in different versions of the empirical diffusion model of CR propagation.

On the “microscopic level” the diffusion of CR results from particle scattering on random MHD waves and discontinuities. The effective “collision integral” for charged energetic particles moving in a magnetic field with small random fluctuations $\delta B \ll B$ can be taken from the standard quasi-linear theory of plasma turbulence (51). The wave-particle interaction is of resonant character so that an energetic particle is predominantly scattered by those irregularities of magnetic field which have their projection of the wave vector on the average magnetic field direction equal to $k_{\parallel} = \pm s/(r_g\mu)$, where μ is the particle pitch angle. The integers $s = 0, 1, 2, \dots$ correspond to cyclotron resonances of different orders. The efficiency of scattering depends on the polarization of the waves and on their distribution in \mathbf{k} -space. The first-order resonance $s = 1$ is the most important for the isotropic and also for the one-dimensional distribution of random MHD waves along the average magnetic field. In some cases – for calculation of scattering at small μ and for calculation of perpendicular diffusion – the broadening of resonances and magnetic mirroring effects should be taken into account. The resulting spatial diffusion is strongly anisotropic locally and goes predominantly along the magnetic field lines. However, strong fluctuations of magnetic field on large scales $L \sim 100 \text{ pc}$, where the strength of the random field is several times higher than the average field strength, lead to the isotropization of global CR diffusion in the Galaxy. The rigorous treatment of this effect is not

trivial, since the field is almost static and the strictly one-dimensional diffusion along the magnetic field lines does not lead to non-zero diffusion perpendicular to \mathbf{B} , see (52) and the references cited there.

Following several detailed reviews of the theory of CR diffusion (53; 54; 8; 14) the diffusion coefficient at $r_g < L$ can be roughly estimated as $D_{xx} \approx (\delta B_{\text{res}}/B)^{-2} v r_g/3$, where δB_{res} is the amplitude of random field at the resonant wave number $k_{\text{res}} = 1/r_g$. The spectral energy density of interstellar turbulence has a power law form $w(k)dk \sim k^{-2+a}dk$, $a = 1/3$ over a wide range of wave numbers $1/(10^{20} \text{ cm}) < k < 1/(10^8 \text{ cm})$, see (6), and the strength of the random field at the main scale is $\delta B \approx 5 \mu\text{G}$. This gives an estimate of the diffusion coefficient $D_{xx} \approx 2 \times 10^{27} \beta R_{\text{GV}}^{1/3} \text{ cm}^2 \text{ s}^{-1}$ for all CR particles with magnetic rigidities $R < 10^8 \text{ GV}$, in a fair agreement with the empirical diffusion model (the version with distributed reacceleration). The scaling law $D_{xx} \sim R^{1/3}$ is determined by the value of the exponent $a = 1/3$, typical for a Kolmogorov spectrum. Theoretically (55) the Kolmogorov type spectrum might refer only to some part of the MHD turbulence which includes the (Alfvénic) structures strongly elongated along the magnetic-field direction and which are not able to provide the significant scattering and required diffusion of cosmic rays. In parallel, the more isotropic (fast magnetosonic) part of the turbulence, with a smaller value of random field at the main scale and with the exponent $a = 1/2$ typical for the Kraichnan type turbulence spectrum, may exist in the interstellar medium (56). The Kraichnan spectrum gives a scaling $D_{xx} \sim R^{1/2}$ which is close to the high-energy asymptotic form of the diffusion coefficient obtained in the ‘plain diffusion’ version of the empirical propagation model. Thus the approach based on kinetic theory gives a proper estimate of the diffusion coefficient and predicts a power-law dependence of diffusion on magnetic rigidity, but the determination of the actual diffusion coefficient has to be done with the help of empirical models of CR propagation in the Galaxy.

2.4 Convection

While the most frequently considered mode of CR transport is diffusion, the existence of galactic winds in many galaxies suggests that convective (or advective) transport could be important. Winds are common in galaxies and can be CR driven (57). CR play a dynamical role in galactic halos (58; 59). Convection not only transports CR, it can also produce adiabatic energy losses as the wind speed increases away from the disk. Convection was first considered by (60) and followed up by (61; 62; 63; 64; 65). Both 1-zone and 2-zone models have been studied: a 1-zone model has convection and diffusion everywhere, a 2-zone model has diffusion alone up to some distance from the plane, and diffusion plus convection beyond.

A recent AnnRev on galactic winds (66) does not mention CR, surprisingly. In the same volume, Cox’s article on the Three Phase Interstellar Medium (5) includes CR as a basic component. Direct evidence for winds in our own Galaxy seems to be confined to the Galactic centre region from X-ray images. However Cox (5) is not sure there is a wind: ‘A Galactic wind may be occurring, but I do not believe that it carries off a significant fraction of the supernova power from the Solar Neighborhood because it would carry off a similar power in the pervading cosmic rays...’

For *one-zone* diffusion/convection models a good diagnostic is the energy-

dependence of the secondary-to-primary ratio: a purely convective transport would have no energy dependence (apart from the velocity-dependence of the reaction rate), contrary to what is observed. If the diffusion rate decreases with decreasing energy, any convection will eventually take over and cause the secondary-to-primary ratio to flatten at low energy: this is observed but convection (proposed (64) to explain just this effect) does not reproduce e.g. B/C very well (67). Another test is provided by radioactive isotopes which effectively constrain the wind speed to $<10 \text{ km s}^{-1} \text{ kpc}^{-1}$ for a speed increasing linearly with distance from the disk (67). A value of $\approx 15 \text{ km s}^{-1}$ (constant speed wind) is required to fit B/C even in the presence of reacceleration according to (68) which can be compared to 30 km s^{-1} in the wind model of (69); the latter value implies an energy dependence of the diffusion coefficient which may conflict with CR anisotropy.

(33) studied a self-consistent *two-zone* model with a wind driven by CR and thermal gas in a rotating Galaxy. The CR propagation is entirely diffusive in a zone $|z| < 1 \text{ kpc}$, and diffusive-convective outside. CR reaching the convective zone do not return, so it acts as a halo boundary with height varying with energy and Galactocentric radius. It is possible to explain the energy-dependence of the secondary-to-primary ratio with this model, and it is also claimed to be consistent with radioactive isotopes. The effect of a Galactic wind on the radial CR gradient has been investigated (70); they constructed a self-consistent model with the wind driven by CR, and with anisotropic diffusion. The convective velocities involved in the outer zone are large (100 km s^{-1}) but this model is still consistent with radioactive CR nuclei which set a much lower limit (67), since this limit is only applicable in the inner zone. Observational support of such models would require direct evidence for a Galactic wind in the halo.

2.5 Reacceleration

In addition to spatial diffusion, the scattering of CR particles on randomly moving MHD waves leads to stochastic acceleration which is described in the transport equation as diffusion in momentum space with some diffusion coefficient D_{pp} . One can estimate it as $D_{pp} = p^2 V_a^2 / (9D_{xx})$ where the Alfvén velocity V_a is introduced as a characteristic velocity of weak disturbances propagating in a magnetic field, see (8; 14) for rigorous formulas.

Distributed acceleration in the entire Galactic volume cannot serve as the main mechanism of acceleration of CR at least in the energy range $1 - 100 \text{ GeV/n}$. In this case the particles of higher energy would spend longer in the system, which would result in an increase of the relative abundance of secondary nuclei as energy increases, contrary to observation. This argument does not hold at low energies where distributed acceleration may be strong and it may explain the existence of peaks in the ratios of secondary to primary nuclei at about 1 GeV/n if the distributed acceleration becomes significant at this energy. The process of distributed acceleration in the interstellar medium is also referred to as ‘reacceleration’ to distinguish it from the primary acceleration process which occurs in the CR sources. It has been shown (71; 46) that the observed dependence of abundance of secondary nuclei on energy can be explained in the model with reacceleration if the CR diffusion coefficient varies as a single power law of rigidity $D_{xx} \sim R^a$ with an exponent $a \sim 0.3$ over the whole energy range (corresponding to particle scattering on MHD turbulence with a Kolmogorov spectrum), and if

the Alfvén velocity is $V_a \sim 30 \text{ km s}^{-1}$, which is close to its actual value in the interstellar medium.

In addition to stable secondary nuclei, the secondary K-capture isotopes are useful for the study of possible reacceleration in the interstellar medium (72). The isotopes ^{37}Ar , ^{44}Ti , ^{49}V , ^{51}Cr and some others decay rapidly by electron capture at low energies where energetic ions can have an orbital electron. The probability to have an orbital electron depends strongly on energy and because of this the abundance of these isotopes and of their decay products are strong functions of energy and sensitive to changes of particle energy in the interstellar medium. The first measurements of an energy-dependent decay of ^{49}V and ^{51}Cr in CR (73) were used to test the rate of distributed interstellar reacceleration (74) but refinement of nuclear production cross sections is required to draw definite conclusions.

The gain of particle energy in the process of reacceleration is accompanied by a corresponding energy loss of the interstellar MHD turbulence. According to calculations (75) the dissipation on CR may significantly influence the Kraichnan nonlinear cascade of waves at less 10^{13} cm and even terminate the cascade at small scales. This results in a self-consistent change of the rigidity dependence of diffusion coefficient with a steep rise of D_{xx} to small rigidities. The scheme explains the high-energy scaling of diffusion $D_{xx} \sim R^{0.5}$ and offers an explanation of the observed energy dependence of primary to secondary ratios.

As mentioned above, the data on secondary nuclei provide evidence against strong reacceleration in the entire Galaxy at $1 - 100 \text{ GeV/n}$. However, the spectra of secondaries can be considerably modified due to processes in the source regions, with a small total Galactic volume filling factor, for the regions where the high-velocity SNR shocks accelerate primary CR. Two effects could be operating there and both lead to the production of a component of secondaries with flat energy spectra (76; 77). One effect is the production of secondaries in SNR by the spallation of primary nuclei which have a flat source energy spectrum close to E^{-2} . Another effect is the direct acceleration by strong SNR shocks of background secondary nuclei residing in the interstellar medium; again the secondaries acquire the flat source energy spectrum. Calculations (77) showed that these effects might produce a flat component of secondary nuclei rising above the standard steep spectrum of secondaries at energies above about 100 GeV/n .

2.6 Galactic structure

Almost all aspects of Galactic structure affect CR propagation, but the most important are the gas content for secondary production and the interstellar radiation field and magnetic field for electron energy losses. The magnetic field is clearly also important for diffusion but the precise absolute magnitude and large-scale structure are less important (at least for CR below 10^{15} eV) than the turbulence properties.

The distribution of atomic hydrogen is reasonably well known from 21-cm surveys, but the molecular hydrogen is less well known since it has to use the CO molecular tracer and the conversion factor is hard to determine and may depend on position in the Galaxy. In fact CR-gas interactions provide one of the best methods to determine the molecular hydrogen content of the Galaxy, because of its basic simplicity, as we describe in the chapter on gamma rays. For more details we refer to another review (78).

The Galactic magnetic field can be determined from pulsar rotation and dispersion measures combined with a model for the distribution of ionized gas. A large-scale field of a few μG aligned with spiral arms exists, but there is no general agreement on the details (79). One recent analysis gives a bisymmetric model for the large-scale Galactic magnetic field with reversals on arm-interarm boundaries (80). Independent estimates of the strength and distribution of the field can be made by simultaneous analysis of radio synchrotron, CR and γ -ray data, and these confirm a value of a few μG , increasing towards the inner Galaxy (81). A lot of effort has gone into constructing magnetic field models to study propagation at energies $>10^{15}$ eV where the Larmor radius is large enough for the global topology to be important; this is relevant to CR anisotropy and the search for point sources. Since this is excluded from our review we refer the reader to (82; 83; 84).

The interstellar radiation field (ISRF) comes from stars of all types and is processed by absorption and re-emission by interstellar dust; it extends from the far-infrared through optical to the UV. Computing the ISRF is difficult, but a great deal of new information on the stellar content of the Galaxy and dust is now available to make better models for use in propagation codes (85).

The local environment around the Sun (86) is also important, for example the local bubble can have an effect on radioactive nuclei as described in Sec 3.2. Extensive coverage of the local environment including CR is in (87).

2.7 Interactions

This large subject is well covered in the literature. Details of the essential processes with references have been conveniently collected in our series of papers: energy losses of nuclei and electrons (67), bremsstrahlung and synchrotron emission (81), inverse-Compton emission including anisotropic scattering (88), pion production of γ -rays, electrons and positrons (39). Pion production has recently been studied in great detail using modern particle-physics codes (89; 90), the former giving spectra harder by 0.05 in the index and γ -ray yields somewhat higher at a few GeV than older treatments. New more accurate parameterizations will be important for the new generation of CR and γ -ray experiments. A useful guide to spallation cross-section measurements and models is the contribution by J. Connell in (91), and a summary of recent advances is in (92; 93; 94). Accounts of radioactive and K-capture processes are in (95; 96; 97; 73; 98).

2.8 Weighted Slabs and Leaky Boxes

As mentioned at the start of this section, at present we believe that the diffusion model with possible inclusion of convection provides the most adequate description of CR transport in the Galaxy at energies below about 10^{17} eV. The closely related leaky-box and weighted slab formalisms have provided the basis for most of the literature interpreting CR data.

In the leaky-box model, the diffusion and convection terms are approximated by the leakage term with some characteristic escape time of CR from the Galaxy. The escape time τ_{esc} may be a function of particle energy (momentum), charge, and mass number if needed, but it does not depend on the spatial coordinates. There are two cases when the leaky box equations can be obtained as a correct approximation to the diffusion model: 1) the model with fast CR diffusion in the

Galaxy and particle reflection at the CR halo boundaries with some probability to escape (9), 2) the formulae for CR density in the Galactic disk in the flat halo model ($z_h \ll R$) with thin source and gas disks ($z_{gas} \ll z_h$) which are formally equivalent to the leaky-box model formulae in the case when stable nuclei are considered (10). The nuclear fragmentation is actually determined not by the escape time τ_{esc} but rather by the escape length in g cm^{-2} : $x = v\rho\tau_{esc}$, where ρ is the average gas density of interstellar gas in a galaxy with the volume of the cosmic ray halo included.

The solution of a system of coupled transport equations for all isotopes involved in the process of nuclear fragmentation is required for studying CR propagation. A powerful method, the weighted-slab technique, which consists of splitting the problem into astrophysical and nuclear parts was suggested for this problem (99; 9) before the modern computer epoch. The nuclear fragmentation problem is solved in terms of the slab model wherein the CR beam is allowed to traverse a thickness x of the interstellar gas and these solutions are integrated over all values of x weighted with a distribution function $G(x)$ derived from an astrophysical propagation model. In its standard realization (100; 101) the weighted-slab method breaks down for low energy CR where one has strong energy dependence of nuclear cross sections, strong energy losses, and energy dependent diffusion. Furthermore, if the diffusion coefficient depends on the nuclear species the method has rather significant errors. After some modification (102) the weighted-slab method becomes rigorous for the important special case of separable dependence of the diffusion coefficient on particle energy (or rigidity) and position with no convective transport. The modified weighted-slab method was applied to a few simple diffusion models in (69; 74). The weighted-slab method can also be applied to the solution of the leaky-box equations. It can easily be shown that the leaky-box model has an exponential distribution of path lengths $G(x) \propto \exp(-x/X)$ with the mean grammage equal to the escape length X .

In a purely empirical approach, one can try to determine the shape of the distribution function $G(x)$ which best fits the data on abundances of stable primary and secondary nuclei (1). It has been established that the shape of $G(x)$ is close to exponential: $G(x) \propto \exp(-x/X(R, \beta))$, and this justifies the use of the leaky-box model in this case. There are several recent calculations of $G(x)$ (103; 104; 69; 74).

The possible existence of truncation, a deficit at small path lengths (below a few g cm^{-2} at energies near 1 GeV/n), relative to an exponential path-length distribution, has been discussed for decades (1; 101; 105; 106). The problem was not solved mainly because of cross-sectional uncertainties. In a consistent theory of CR diffusion and nuclear fragmentation in the cloudy interstellar medium, the truncation occurs naturally if some fraction of CR sources resides inside dense giant molecular clouds (107).

For radioactive nuclei, the classical approach is to compute the ‘surviving fraction’ which is the ratio of the observed abundance to that expected in the case of no decay. Often the result is given in the form of an effective mean gas density, to be compared with the average density in the Galaxy, but this density should not be taken at face value. The surviving fraction can better be related to physical parameters (108). None of these methods can face the complexities of propagation of CR electrons and positrons with their large energy and spatially dependent energy losses.

2.9 Explicit models

Finally the mathematical effort required to put the 3-D Galaxy into a 1-D formalism becomes overwhelming, and it seems better to work in physical space from the beginning: this approach is intuitively simple and easy to interpret. We can call these ‘explicit solutions.’ The explicit solution approach including secondaries was pioneered by (10) and applied to newer data by (109; 65) with analytical solutions for 2D diffusion-convection models with a cosmic-ray source distribution, which however had many restrictive approximations to make them tractable (no energy losses, simple gas model). More recently a semi-empirical model which is 2D and includes energy-losses and reacceleration has been developed (110; 68). This is a closed-form solution expressed as a Green’s function to be integrated over the sources. It incorporates a radial CR source distribution, but the gas model is a simple constant density within the disk. (111) give an analytical solution for the time-dependent case with a generalized gas distribution but now *without energy losses*. (This shows again the problem of handling both gas and energy losses simultaneously in analytical schemes).

A ‘myriad sources model’ (112), which is actually a Green’s function method without energy losses, yields similar results to (113) for the diffusion coefficient and halo size. But applying the no-energy loss case to ACE data is not really justified, and some defects in their formulation have been pointed out (111). A 3D analytical propagation method has been developed (114; 115) with energy loss and reacceleration, going via a PLD, but it cannot handle ionization losses properly, see section 2.2 of (115). They have no spatial boundaries at all and rather simplified (exponential) forms for the gas and other distributions. An approach adapted to fine-scale spatial and temporal variations has been described (116). This uses a Green’s function without energy losses or detailed gas model and hence is limited in its application, but is useful for studying the effect of discrete sources.

The most advanced explicit solution to date is the fully numerical model described in the next section. Even this has limitations in treating some aspects (e.g. when particle trajectories become important at high energies) so one might ask whether a fully Monte-Carlo approach (as is commonly done for energies $> 10^{15}$ eV) would not be better in the future, given increasing computing power. This would allow effects like field-line diffusion (important for propagation perpendicular to the Galactic plane) to be explicitly included. However it is still challenging: a GeV particle diffusing with a mean free path of 1 pc in a Galaxy with 4 kpc halo height takes $\sim (4000/1)^2 \approx 10^7$ scatterings to leave the Galaxy, which would even now need supercomputers to obtain adequate statistics. Hence we expect numerical solution of the propagation equations to remain an important approach for the foreseeable future.

2.10 GALPROP

The GALPROP code (67) was created with the following aims: 1. to enable simultaneous predictions of all relevant observations including CR nuclei, electrons and positrons, γ -rays and synchrotron radiation, 2. to overcome the limitations of analytical and semi-analytical methods, taking advantage of advances in computing power, as CR, γ -ray and other data become more accurate, 3. to incorporate current information on Galactic structure and source distributions, 4. to pro-

vide a publicly-available code as a basis for further expansion. The first point is the most important, the idea being that all data relate to the same system, the Galaxy, and one cannot for example allow a model which fits secondary/primary ratios while not fitting γ -rays or not being compatible with the known interstellar gas distribution. There are many simultaneous constraints, and to find one model satisfying all of them is a challenge, which in fact has not been met up to now. Upcoming missions should benefit².

We give a very brief summary of GALPROP; for details we refer the reader to the relevant papers (67; 39; 81; 117; 113; 75) and a dedicated website³. The propagation equation (1) is solved numerically on a spatial grid, either in 2D with cylindrical symmetry in the Galaxy or in full 3D. The boundaries of the model in radius and height, and the grid spacing, are user-definable. In addition there is a grid in momentum; momentum (not e.g. kinetic energy) is used because it is the natural quantity for propagation in equation (1). Parameters for all processes in equation (1) can be controlled on input. The distribution of CR sources can be freely chosen, typically to represent SNR. Source spectral shape and isotopic composition (relative to protons) are input parameters. Interstellar gas distributions are based on current HI and CO surveys, and the interstellar radiation field is based on a detailed calculation. Cross-sections are based on extensive compilations and parameterizations (92). The numerical solution proceeds in time until a steady-state is reached; a time-dependent solution is also an option. Starting with the heaviest primary nucleus considered (e.g. ^{64}Ni) the propagation solution is used to compute the source term for its spallation products, which are then propagated in turn, and so on down to protons, secondary electrons and positrons, and antiprotons. In this way secondaries, tertiaries etc. are included. (Production of ^{10}B via the ^{10}Be -decay channel is important and requires a second iteration of this procedure.) GALPROP includes K-capture and electron stripping processes, where a nucleus with an electron (H-like) is considered a separate species because of the difference in the lifetime. Since H-like atoms have only one K-shell electron, the K-capture decay half-life has to be increased by a factor of 2 compared to the measured half-life value. Primary electrons are treated separately. Normalization of protons, helium and electrons to experimental data is provided (all other isotopes are determined by the source composition and propagation). γ -rays and synchrotron are computed using interstellar gas data (for pion-decay and bremsstrahlung) and the ISRF model (for inverse Compton). Spectra of all species on the chosen grid and the γ -ray and synchrotron skymaps are output in a standard astronomical format for comparison with data. Recent extensions to GALPROP include non-linear wave damping (75) and a dark matter package.

The computing resources required by GALPROP are moderate by today's standards. We remark that while GALPROP has the ambitious goal of being 'realistic', it is obvious that any such model can only be a crude approximation to reality. Some known limitations are: only energies below 10^{15} eV (no trajectory calculations), uniform source abundances (no superbubble enhancements), only scales >10 pc (no clumpy ISM: limited by computer power), B-field treated as random for synchrotron (regular component affects structure of radio emission).

²GALPROP has been adopted as the standard for diffuse Galactic γ -ray emission for NASA's GLAST γ -ray observatory, and is also made use of by the AMS, ACE, HEAT and Pamela collaborations.

³<http://galprop.stanford.edu>

For these cases other techniques may be more appropriate, and they provide a goal for future developments of GALPROP.

2.11 Numerical versus analytical

The following expresses the authors' opinion on this matter. The analytical approaches are claimed to have various advantages as follows:

1. **Physical insight:** of course it is true that analytical solutions for simple cases are very useful to get insight into the relations between the quantities involved, and for rough estimates. In fact the analytical formulae may become so complicated that finally no insight is gained. In contrast the numerical models are very intuitive since they generate explicitly the CR distribution over the Galaxy for all species.
2. **Equivalent to full solution of propagation equation:** only true under restrictive conditions, especially involving energy-losses and spatially varying densities. Electrons and positrons are anyway beyond analytical methods (for energy-losses on realistic interstellar radiation fields), while these are an essential component of the CR.
3. **Faster, easier to compute:** with today's computers the speed issue has become irrelevant, and the implementation of a numerical model is not harder than the complicated integrals over Bessel functions etc.

In summary we can do no better than a quotation from a paper of 26 years ago (!) (118): 'It is unclear whether one would wish to go much beyond the generalizations discussed above for an analytically soluble diffusion model. The added insight from any analytic solution over a purely numerical approach is quickly cancelled by the growing complexity of the formulae. With rapidly developing computational capabilities, one could profitably employ numerical solutions...' We remark also that for CR air-shower calculations, analytical methods gave way to numerical ones at least 40 years ago.

2.12 Self-consistent models

A few attempts at a self-consistent description of CR in the Galaxy have been made, including them as a relativistic gas as one component of ISM dynamics. This is obviously much harder than the phenomenological models described above which treat propagation in a prescribed environment. 3D models of the magnetized ISM with a CR-driven wind have been made by (32; 33) and this is claimed to be also consistent with CR secondary/primary ratios. Such a wind has been put forward as a possible explanation of the CR gradient problem (70). The Parker instability has been re-analysed recently (119) using anisotropic diffusion (120) and followed by a CR-driven Galactic dynamo model (121) which uses an extension the Zeus-3D MHD code (30) including CR propagation and sources. CR propagation in a magnetic field produced by dynamo action of a turbulent flow (31) presents the whole subject from a novel viewpoint. The extension of such approaches to include CR spectra, secondaries, γ -rays etc., which would provide a complete set of comparisons with observations, would be very desirable but has not yet been attempted. Another kind of self-consistency is to include the effect of CR on the diffusion coefficient (75) as described in more detail in Section 2.5.

3 Confrontation of Theory with Data

3.1 Stable secondary/primary ratios

The reference ratio is almost always B/C because B is entirely secondary, the measurements are better than for other ratios and are available up to 100 GeV. Because C,N,O are the major progenitors of B, the production cross sections are better known than, e.g. in the case of Be and Li (122; 94).

The usual procedure is to use a leaky-box or weighted-slab formalism with the empirical rigidity-dependence $X(R) = (\beta/\beta_0)X_0$, $(\beta/\beta_0)(R/R_0)^{-\alpha}X_0$ for $R < R_0$, $R > R_0$ respectively. The break at R_0 is required because B/C is observed to decrease to low energies faster than the β -dependence (which just describes the velocity effect on the reaction rate). The source composition depends on the form and parameters of $X(R)$, and vice-versa, (since for example B is produced by C,N,O etc) so the procedure is iterative, starting from a solar-like composition.

A typical parameter set fitting the data (69) is $\alpha = 0.54$, $X_0 = 11.8 \text{ g cm}^{-2}$, $R_0 = 4.9 \text{ GV/c}$, with a source spectrum rigidity index -2.35 . In principle all other secondary/primary ratios should be consistent with the same parameter set. This is generally found to be the case. As a state-of-the-art application of the weighted slab technique of (102) we again refer to (69). This is applicable to stable nuclei only but includes energy losses and gains subject to the limitations described in Section 2.8. They apply the method to 1-D disk-halo diffusion, convection, turbulent diffusion and reacceleration models cast in weighted-slab form. Fig. 8 shows B/C and (Sc+Ti+V)/Fe, so-called sub-Fe/Fe, from their paper. Clearly the models cannot be distinguished based on these types of data alone, and they can all provide an adequate fit; this shows the importance of using other species as well as the ones used here. The models can be used to obtain the injection spectrum of primaries, and they find an index of 2.3 to 2.4 for C and Fe in the energy range 0.5 – 100 TeV, with the propagated spectrum and data shown in Fig. 9.

It has been claimed that no break in $X(R)$ is required to fit Voyager 2 outer-heliosphere B/C, N/O and sub-Fe/Fe data extended to 1.5 GeV, plus HEAO3 data, and adopting suitable solar modulation levels (123). Voyager 2 provides a unique dataset because of the low solar modulation.

We consider now *explicit* models in the sense of Section 2.9. Basically the same procedure is adopted, with $D_{xx}(R)$ replacing $X(R)$. Again an ad-hoc break in $D_{xx}(R)$ is required in the absence of other mechanisms. Because of the unphysical nature of such a $D_{xx}(R)$, many attempts to find a better explanation have been made, including convection, reacceleration/wave damping, and local sources.

Convection implies an energy-independent escape from the Galaxy so that it dominates at low energies as the diffusion rate decreases, so it gives a simple low-energy asymptotic $X(R) \propto \beta$. However this does not resemble the observed B/C energy-dependence, being too monotonic (67). Furthermore quite severe limits on the convection velocity come from unstable nuclei.

Reacceleration affects the secondary-primary ratio as described in Section 2.5. Many papers have shown how B/C and other ratios can be reproduced with reacceleration at a plausible level and no ad-hoc break in the diffusion coefficient. An example is shown in Fig. 8. An application including recent ACE (Li, Be, B, C) data is in (94). Since reacceleration at some level *must* be present if diffusion occurs on moving scatterers (e.g. Alfvén waves) this mechanism is favoured but

it is not proven. Direct evidence for reacceleration could come from certain K-capture nuclei (Section 3.4). Reacceleration requires a smaller value of α , typically 0.3 – 0.4, consistent with Kolmogorov turbulence, which helps solve the problems with anisotropy (section 3.5).

Closely related to reacceleration is wave-damping as described in Section 2.5. This can reproduce B/C, protons and antiprotons satisfactorily as shown in Fig. 10, and also other data (75). The result of this process is a very sharp rise of the diffusion coefficient at rigidities less than about 1.5 GV. The Kolmogorov-type dependence is not very successful in this scheme, while a Kraichnan-type works better with a high rigidity asymptotic $D \sim R^{0.5}$ (first panel in Fig. 10).

A quite different set of parameters has been proposed (68): $\alpha = 0.7 - 0.9$ and injection index ≈ 2.0 , based on fitting many species simultaneously, and is suggested to produce the B/C low-energy decrease from convection. Such a large α would give problems for the anisotropy (Section 3.5). A related analysis (110) claims to exclude the Kolmogorov-type spectrum.

An alternative explanation for the falloff in B/C at low energies invokes weakly nonlinear (in contrast to quasi-linear) transport theory of cosmic rays in turbulent Galactic magnetic fields (124; 125).

Another, simpler, explanation of the B/C energy-dependence is the local-source model (104; 126) in which part of the primary CR have an additional local component. Since the secondary flux has to come from the Galaxy-at-large (the local secondaries being negligible) a steep local primary source will cause B/C to decrease at low energies. The known existence of the local bubble containing the Sun, and its probable origin in a few supernovae in the last few million years, make this a plausible possibility, but hard to prove or disprove. It is claimed (104) that if B/C is fitted in such a model, then sub-Fe/Fe is not fitted, but an acceptable fit to this and other data *is* found in (126) using a diffusion model for the large-scale component.

3.2 Unstable secondary/primary ratios: ‘radioactive clocks’

The five unstable secondary nuclei which live long enough to be useful probes of cosmic-ray propagation are ^{14}C , ^{10}Be , ^{26}Al , ^{36}Cl and ^{54}Mn , with properties summarized in (101; 127; 126). ^{10}Be is the longest-lived and best measured. The theory is presented in section 2.2. Based on these isotopes and updated cross-sections (128) find $z_h = 4-6$ kpc, consistent with their earlier estimates of 3–7 kpc (98) and 4–12 kpc (67). Fig. 11 shows a comparison of $^{10}\text{Be}/^9\text{Be}$ with models; the ISOMAX ^{10}Be measurements (129) up to 2 GeV (and hence longer decay lifetime) are consistent with the fit to the other data, although the statistics are not very constraining.

The data are often interpreted in terms of the leaky-box model, but this is misleading (108; 131; 127). For the formulae and the detailed procedure for the leaky-box model interpretation see (132). Luckily the leaky-box model surviving fraction can be converted to a physically meaningful quantities (131) for a given model; for example in a simple diffusive halo model, the surviving fraction determines the diffusion coefficient, which can be combined with stable secondary/primary ratios to derive the halo size. Typical results are $D_{xx} = (3 - 5) \times 10^{28} \text{ cm}^2 \text{ s}^{-1}$ (at 3 GV) and $z_h = 4$ kpc. We can then compare the leaky-box model ‘escape time’ $\approx 10^7$ yr with the actual time for CR to reach the halo boundary after leaving their sources, the latter being typically an order

of magnitude larger. The leaky-box model ‘gas density’ is typically 0.3 cm^{-3} compared to the actual average density 0.03 cm^{-3} for a 4 kpc halo height, again an order-of-magnitude difference.

Since radioactive secondaries only travel a few hundred pc before decaying it is sometimes considered (133) that they cannot give information on the propagation region of CR; this is somewhat misleading since it is precisely the *combination* of stable and radioactive data which *does* allow this; the radioactives determine the diffusion coefficient, which then allows the size of the full propagation region to be determined from the stable secondary/primary ratio (where the CR do come from the entire containment region). This of course assumes the diffusion coefficient does not vary greatly from the local region to the full volume.

The effect of the local bubble surrounding the Sun on the interpretation of radioactive nuclei was pointed out by (127). The flux of unstable secondaries is reduced if they are not produced in a gas-depleted region around the Sun, since they will decay before reaching us, and this could lead to an overestimate of the halo size if interpreted in a simple diffusive halo model. This effect would be reduced if the diffusion coefficient in the local region were larger than the large-scale value. In fact the situation is even more complex. According to (86; 87; 134) the Sun left the local bubble about 10^5 years ago after spending several million years inside, and we now live in the CLIC (collection of local interstellar clouds) with HI density about 0.2 cm^{-3} and 35 pc extent. This aspect of the problem for CR propagation has not yet been addressed.

3.3 K-capture isotopes and acceleration delay

Three isotopes produced in explosive nucleosynthesis decay essentially only by K-capture: ^{59}Ni ($7.6 \times 10^4 \text{ y}$), ^{57}Co (0.74 yr), ^{56}Ni (6d). If acceleration occurs before decay, the decay will be suppressed since the nuclei are stripped. ^{56}Ni is absent as expected, but the other two nuclei are more interesting. (135) used ACE data on these nuclei to show that the delay between synthesis and acceleration is long compared with the ^{59}Ni decay-time, unless significant ^{59}Co is synthesised in supernovae; considering theoretical ^{59}Co yields they conclude on a delay $\geq 10^5 \text{ y}$. This is inconsistent with models in which supernova accelerate their own ejecta, but consistent with acceleration of existing interstellar material. The possibility of in-flight electron attachment complicates the analysis however (135). For more discussion see (133). A result from TIGER on Co/Ni at 1-5 GeV/n (136) supports the acceleration delay also at higher energies.

3.4 K-capture isotopes and reacceleration

Analyses using ACE data for ^{49}V , ^{51}V , ^{51}Cr , ^{52}Cr and ^{49}Ti and other nuclei have been made (73), (137), (74). (137) found that while $^{51}\text{V}/^{52}\text{Cr}$ was in better agreement with reacceleration models, $^{49}\text{Ti}/^{46+47+48}\text{Ti}$ gave the opposite result. (74) find that while V/Cr ratios are in slightly better agreement with models including reacceleration, the ratios involving Ti are inconclusive. (137) used ACE data on ^{37}Ar , ^{44}Ti , ^{49}V , ^{51}Cr , ^{55}Fe and ^{57}Co , with inconclusive results. The main problem is the accuracy of the fragmentation cross-sections (126). Discussion of ACE and previous results can be found in section 3 of (133).

3.5 Anisotropy

High isotropy is a distinctive quality of Galactic CR observed at the Earth. The global leakage of CR from the Galaxy and the contribution of individual sources lead to anisotropy but the trajectories of energetic charged particles are highly tangled by regular and stochastic interstellar magnetic fields which isotropize the CR angular distribution. This makes difficult or even impossible the direct association of detected CR particles with their sources, except for the highest energy particles. Observations give the amplitude of the first angular harmonic of anisotropy at the level of $\delta \sim 10^{-3}$ in the energy range 10^{12} to 10^{14} eV where the most reliable data are available, see (138; 139) and Fig. 12. The angular distribution of particles at lower energies is significantly modulated by the solar wind. The statistics at higher energies are not good enough yet but the measurements indicate the anisotropy amplitude at a level of a few percent at $10^{16} - 10^{18}$ eV. The data of the Super-Kamiokande-I detector (140) allowed accurate two-dimensional mapping of CR anisotropy at 10^{13} eV (see also the Tibet Air Shower Array results (138)). After correction for atmospheric effects, the deviation from the isotropic event rate is 0.1% with a statistical significance of $>5\sigma$ and direction to maximum excess at roughly $\alpha = 75^\circ$, $\delta = -5^\circ$.

The amplitude of anisotropy in the diffusion approximation is given by the following equation which includes pure diffusion and convection terms: $\delta = -[3D\nabla f + \mathbf{up}(\partial f/\partial p)]/vf$, see (8). Here D is the diffusion tensor, and it is assumed that the magnetic inhomogeneities which scatter CR particles are frozen in the background medium, moving with velocity $u \ll v$, which gives rise to the convection term (also called the Compton-Getting term).

The Compton-Getting anisotropy is equal to $(\gamma + 2)u/c$ for ultra-rerelativistic CR with a power law spectrum $I(E) \sim p^2 f(p) \sim E^{-\gamma}$. The motion of the Solar System through the local interstellar medium produces the constant term in the energy-dependence of the anisotropy $\sim 4 \times 10^{-4}$, with a maximum intensity in the general direction to the Galactic centre region, which does not agree with the data at $10^{12} - 10^{14}$ eV which point to an excess intensity from the anticenter hemisphere. The convection effect is outweighed by the diffusion anisotropy which is due to the non-uniform distribution of CR in the Galaxy. The systematic decrease of CR intensity to the periphery of the Galaxy and the CR fluctuations produced by nearby SNR are approximately equally important for the formation of the local CR gradient.

Calculations of CR anisotropy (141) are illustrated in Fig. 12 where the effect of global leakage from the Galaxy and the overall contribution of known SNR with distances up to 1 kpc are shown separately. Two basic versions of the flat-halo diffusion model – the plain diffusion model with $D \sim E^{0.54}$ and the model with reacceleration where $D_{xx} \sim E^{0.3}$ – were used in the calculations. The values of D_{xx} were taken from (69). The diffusion from a few nearby SNR with different ages and distances results in a non-monotonic dependence of anisotropy on energy. The flux from the Vela SNR probably dominates over other SNR at energies below about 6×10^{13} eV in the plain diffusion model and below about 10^{14} eV for the model with reacceleration. The results of these calculations indicate that the diffusion model with reacceleration is compatible with the data on CR anisotropy within a factor of about 3. On the other hand it seems that the plain diffusion model with its relatively strong dependence of diffusion on energy predicts a too large anisotropy at $E > 10^{14}$ eV. It should be stressed that CR diffusion is here

assumed to be isotropic, which is a seriously simplifying assumption but which is difficult to avoid because of the complicated and in fact unknown detailed structure of the Galactic magnetic field. The presence of a large-scale random magnetic field justifies the approximation of isotropic diffusion on scales larger than a few hundred parsecs, but the anisotropy is a characteristic which is very sensitive to the local surroundings of the Solar System including the direction of magnetic field and the value of diffusion tensor, see discussion in (8).

3.6 Diffuse Galactic Gamma Rays

Gamma rays (above about 100 MeV) from the interstellar medium hold great promise for CR studies since they originate throughout the Galaxy, not just the local region of direct measurements. The complementarity of γ -rays and direct measurements can be exploited to learn most about CR origin and propagation. Despite this the interpretation has brought surprises in that the γ -ray spectrum is not just as would be expected from the directly-observed CR spectra. γ -rays are produced in the interstellar medium by interactions of CR protons and He (π^0 -decay) and electrons (bremsstrahlung) with gas, and electrons with the interstellar radiation field via inverse-Compton scattering. For details of the processes the reader is referred to (39; 81; 88; 113). Additional astronomical material comes into play like the distribution of atomic and molecular gas, and the interstellar radiation field. In fact γ -rays provide an important independent handle on molecular hydrogen and its relation to its CO molecular tracer, which has taken its place beside more traditional determinations.

Historically observations started with the OSO-III satellite in 1968, followed by SAS-2 in 1972, COS-B (1975–1982) and CGRO (1991–2000). Each of these experiments represented a significant leap forward with respect to its predecessor. SAS-2 established the existence of emission from the interstellar medium and allowed a first attempt to derive the CR distribution. With COS-B the CR distribution could be better derived and it was found not to follow the canonical distribution of supernova remnants, which posed a problem for the SNR origin of CR. A rather dependable value for the CO-H₂ relation was derived. With EGRET and COMPTEL on the Compton Gamma Ray Observatory (CGRO) the improvement in data quality was sufficient to allow such studies to be performed in much greater detail. There is now so much relevant information and theory that a rather ‘realistic’ approach is justified and indeed necessary. At this point the best approach seems to be explicit modelling of the high-energy Galaxy putting in concepts from CR sources and propagation, Galactic structure, etc. The idea of a single model to reproduce both CR and gamma-ray (and other) data simultaneously arose naturally and is the goal of the GALPROP project (see Sec 2.10). For a recent review see (143).

To illustrate the current state of the art, we show spectra and profiles from a recent GALPROP model compared with CGRO/EGRET and COMPTEL data. This is based on (113) and (144) where full details can be found. The first model is based simply on the directly-measured CR spectra together with a radial gradient in the CR sources. It is immediately clear that the spectrum is not well predicted, being below the EGRET data for energies above 1 GeV. However remembering that this is an *unfitted* prediction, it does show that the basic assumption that the γ -rays are produced in CR interactions is correct; the factor 2 differences are telling us something about the remaining uncertainties. The extent to which the

CR spectra have to be modified to get a good fit including the GeV excess is shown in Fig. 13 and the resulting γ -ray model prediction in Fig. 14. The difference between the directly-observed and modified spectra are within plausible limits considering solar modulation and spatial fluctuations in the Galaxy on scales >100 pc. A detailed justification is lacking however, so this so-called ‘optimized’ model is just an existence proof rather than a conclusive result. Other more drastic modifications to the CR spectrum have been proposed (78) as follows:

(i) a very hard electron injection spectrum, which could be allowed invoking large fluctuations due to energy losses and the stochastic nature of supernova remnants in space and time – the solar vicinity is not necessarily a ‘typical’ place for electron measurements to be representative (145; 81). However the variations required are even larger than can reasonably be expected (113), so this model seems unlikely.

(ii) a hard proton spectrum, again invoking spatial variations in the Galaxy so the solar vicinity is not typical; this is more difficult than for electrons since the proton energy-losses are negligible. It turns out this possibility can be ruled out on the basis of antiproton measurements: too many antiprotons would be produced by the same protons which generate the gamma rays (146; 113; 78). A related suggestion invokes the dispersion in the radio spectral indices of SNR, which indicates a dispersion in electron indices and if assumed to apply to CR protons (147) could produce the GeV excess; this should also be tested against antiprotons.

Perhaps a completely different source of the excess GeV gamma rays is present, and the possibility of a dark-matter origin has been pursued (148) but found to produce an excess of CR antiprotons (149). We will not enter this debate here since it is not directly related to the problem of CR propagation. It does however show how essential is a good understanding of the CR-induced γ -rays in the Galaxy for the study of potentially more fundamental physics (150).

The angular distribution of γ -rays provides an essential test for any model. The problem with the large expected gradient from SNR is critical. The distribution of SNR is hard to measure because of selection effects, so this problem could be safely ignored in the past, but now the distribution of pulsars can be determined with reasonable accuracy and this should trace SNR since supernovae are pulsar progenitors. The pulsar gradient is indeed larger than originally deduced from γ -rays as shown in Fig. 15. The distribution of SNR in external galaxies shows a similar gradient to pulsars (152). The problem therefore remains, but a possible solution may be found in another uncertainty, the Galactic distribution of molecular hydrogen. Since we have to rely on the CO tracer molecule, any variation in the relation of CO to H_2 will affect the interpretation of the γ -ray data. (144) noted that there is independent evidence for an increase in the ratio of H_2 to CO with Galactocentric radius, related to Galactic metallicity gradients, and that this can resolve the problem, allowing CR sources to follow the SNR distribution as traced by pulsars. Fig. 16 shows longitude and latitude profiles based on such a model, showing a satisfactory agreement with EGRET data. However the magnitude of the variation in H_2 to CO, or its relation to metallicity and other effects, is uncertain so the issue will need more study. Future data from GLAST will help by giving much finer angular resolution and the possibility of better separating the molecular and atomic hydrogen components. Another possible solution to the gradient puzzle in terms of a radially dependent Galactic wind was proposed by (70) (see Sections 2.4 and 2.12).

Note the large contribution inverse-Compton emission to the spectra and profiles (Figs. 14, 16); this is the reason that the predicted emission is in good agreement with the EGRET data right up to the highest latitudes (where the gas-related pion-decay emission is small). Therefore γ -rays constrain both protons and electrons, the different angular distributions being clearly distinguishable. The high-latitude inverse-Compton emission is independent evidence for the existence of a CR halo extending up to several kpc above the plane, deduced from radioactive CR isotopes as explained in Section 3.2. Interestingly, *secondary electrons and positrons* make a significant contribution to the lower-energy bremsstrahlung and inverse-Compton gamma-rays (113); so we can in principle observe secondaries from all over the Galaxy, complementary to the local direct measurements.

3.7 Antiprotons and positrons

The spectrum and origin of antiprotons in CR has been a matter of active debate since the first reported detections in balloon flights (153; 154). There is a consensus that most of the CR antiprotons observed near the Earth are secondaries (155). Due to the kinematics of secondary production, the spectrum of antiprotons has a unique shape distinguishing it from other cosmic-ray species. It peaks at about 2 GeV, decreasing sharply towards lower energies. In addition to secondary antiprotons there are possible sources of primary antiprotons; those most often discussed are dark matter particle annihilation and evaporation of primordial black holes.

In recent years, new data with large statistics on both low and high energy antiproton fluxes have become available (156; 157; 158; 159; 160; 161; 162) thanks mostly to continuous improvements of the BESS instrument and its systematic launches every 1-2 years. This allows one to test models of CR propagation and heliospheric modulation. Additionally, accurate calculation of the secondary antiproton flux predicts the “background” for searches for exotic signals such as WIMP annihilation.

Despite numerous efforts and overall agreement on the secondary nature of the majority of CR antiprotons, published estimates of the expected flux differ significantly (see, e.g., Fig. 3 in (158)). Calculation of the secondary antiproton flux is a complicated task. The major sources of uncertainties are three-fold: (i) incomplete knowledge of cross sections for antiproton production, annihilation, and scattering, (ii) parameters and models of particle propagation in the Galaxy, and (iii) modulation in the heliosphere. While the interstellar antiproton flux is affected only by uncertainties in the cross sections and propagation models, the final comparison with experiment can only be made after correcting for the solar modulation. Besides, the spectra of CR nucleons have been directly measured only inside the heliosphere while we need to know the spectrum outside, in interstellar space, to compute the antiproton production rate correctly.

It has recently been shown (117) that accurate antiproton measurements during the last solar minimum 1995–1997 (158) are inconsistent with existing propagation models at the $\sim 40\%$ level at about 2 GeV, while the stated measurement uncertainties in this energy range are now $\sim 20\%$. The conventional models based on local CR measurements, simple energy dependence of the diffusion coefficient, and uniform CR source spectra throughout the Galaxy fail to reproduce simultaneously both the secondary to primary nuclei ratio and antiproton flux.

A reacceleration model designed to match secondary to primary nuclei ratios produces too few antiprotons because the diffusion coefficient is too large. Models without reacceleration can reproduce the antiproton flux, but cannot explain the low-energy decrease in the secondary-to-primary nuclei ratios. To be consistent with both, the introduction of breaks in the diffusion coefficient and the injection spectrum is required, which would suggest new phenomena in particle acceleration and propagation. A solution in terms of propagation models requires a break in the diffusion coefficient at a few GeV which has been interpreted as a change in the propagation mode (117). The latter calculation employs a modern steady-state drift model of propagation in the heliosphere to predict the proton and antiproton fluxes near the Earth for different modulation levels and magnetic polarity.

If our local environment influences the spectrum of CR, then it is possible to solve the problem by invoking a fresh “unprocessed” nuclei component at low energies (126), which may be produced in the Local Bubble. The idea is that primary CR like C and O have a local low-energy component, while secondary CR like B are produced Galaxy-wide over the confinement time of 10–100 Myr. In this way an excess of B, which appears when propagation parameters are tuned to match the \bar{p} data, can be eliminated by an additional local source of C (see Section 3.1). The model appears to be able to describe a variety of CR data, but at the cost of additional parameters.

A consistent \bar{p} flux in reacceleration models can be obtained if there are additional sources of protons $\lesssim 20$ GeV (163). This energy is above the \bar{p} production threshold and effectively produces \bar{p} ’s at $\lesssim 2$ GeV. The intensity and spectral shape of this component could be derived by combining restrictions from \bar{p} ’s and diffuse γ -rays.

It is clear that accurate measurements of \bar{p} flux are the key to testing current propagation models. If new measurements confirm the \bar{p} “excess,” current propagation and/or modulation models will face a challenge. If not – it will be evidence that the reacceleration model is currently the best one to describe the data. Here we have to await for the next BESS-Polar flight which should bring much larger statistics, and Pamela (164), currently in orbit.

Positrons in CR were discovered in 1964 (165). The ratio of positrons to electrons is approximately 0.1 above ~ 1 GeV as measured near the Earth. Secondary positrons in CR are mostly the decay products of charged pions and kaons (π^+ , K^+) produced in CR interactions with interstellar gas. The calculation of the positron production by CR generally agrees with the data and indicates that the majority of CR positrons are secondary (166; 39). Some small fraction of positrons may also come from sources (167), such as pulsar winds (168) or WIMP annihilations (169).

In interstellar space the secondary positron flux below ~ 1 GeV is comparable to the electron flux which makes positrons non-negligible contributors to the diffuse γ -ray emission in the MeV range (113). The contribution of secondary positrons and electrons in diffuse Galactic γ -ray emission models essentially improves the agreement with the data, making secondary positrons effectively detectable in γ -rays.

The accuracy of spacecraft and balloon-borne experiments has substantially increased during the last decade. The data taken by various instruments including AMS, CAPRICE and HEAT (170; 41; 171; 172) are in agreement with each other within the error bars, which are however still quite large. A recent measurement

of CR positron fraction by the HEAT instrument (42) indicates an excess (feature) between 5 and 7 GeV at the level of $\sim 3\sigma$ over the smooth prediction of a propagation model (39). When all the HEAT flights are combined, the data show an excess above ~ 8 GeV, with the most significant point at ~ 8 GeV (42). The Pamela satellite (164) currently in orbit, will have a very good positron statistics.

3.8 Electrons and Synchrotron Radiation

CR electrons require a separate treatment from nuclei because of their rapid energy losses and their link with synchrotron radiation. Their low energy density compared with nuclei ($\approx 1\%$) is not yet understood; standard SNR shock acceleration does not predict such a ratio and it is normally a free parameter in models e.g. (173). Direct measurements extend from MeV to TeV ; at low energies solar modulation is so large that the interstellar fluxes are really unknown. At TeV energies the statistics are very poor but new experiments are in progress. Young SNR contain TeV electrons as is shown by their non-thermal X-ray emission, and energies up to 100 TeV are possible (174). The rapid energy losses mean that contributions from old nearby SNR such as Loop 1, Vela, the Cygnus Loop and MonoGem could make an important contribution to the local electron spectrum above 100 GeV and dominate above 1 TeV, see Fig. 4 (37). The rapid energy losses of electrons also produce time- and space-dependent effects described in the next section. The essential propagation effects are seen in Fig. 13; at energies below 1 GeV the interstellar spectrum is flatter than the injection spectrum, due to Coulomb losses; there is an intermediate energy range where the spectrum is similar to that at injection, and at high energies it steepens due to inverse Compton and synchrotron losses and energy-dependent diffusion. For propagation models we need an injection spectrum which reproduces the observations; a typical spectral index is 2.4, similar to nuclei, which produces the observed high-energy slope of 3.3 (113). The synchrotron spectral index is $\beta_\nu = (\gamma - 1)/2$ for an electron index γ ; the observed $\beta_\nu = 0.6 - 1$, increasing with frequency, implies $\gamma = 2.4 - 3$ increasing with energy, in satisfactory agreement. Detailed geometrical models of the Galactic synchrotron emission have been constructed (175; 176). A more physical interpretation requires propagation and magnetic field modelling as for example in (81). Combined with γ -ray data this allows the magnetic field to be determined as a function of Galactocentric radius independent of other techniques (81). Since that work a great deal of new radio data has become available both from new ground-based surveys and from balloons and satellites for cosmology (e.g. WMAP). Since Galactic synchrotron is an essential ‘foreground’ for CMB studies there is a large overlap of interest between these fields. Exploitation of these data for CR studies has only just begun but is expected to accelerate with the forthcoming Planck mission.

Radio continuum observations of other galaxies provide a complementary view of electrons via synchrotron radiation (177; 178). The classical case is the edge-on galaxy NGC891 (179; 180) which has a non-thermal halo extending to several kpc, and this helped to give credence to the idea of a large halo in our Galaxy. More recent observations of this and other edge-on galaxies confirm large halos (181). The spectral index variations due to energy losses provide a test of propagation in principle, although this has not been very fruitful up to now. This effect can also be measured in starburst galaxies (182). Face-on galaxies like M51 show marked spiral structure in the continuum (177), but this is probably mainly a magnetic-

field effect. It is not possible reliably to separate CR and magnetic field variations, although this is often attempted assuming equipartition of energy between CR and field, which although having no firmly established physical basis nevertheless gives field values quite similar to other methods (183; 178).

The tight radio-continuum/far-infrared correlation for galaxies (184; 185; 186) is worth mentioning here. It holds both within galaxies (down to 100 pc or less) and from galaxy to galaxy, and over several orders of magnitude in luminosity; it presumably contains clues to CR origin and propagation. The ‘CR calorimeter’ (187) is the simplest interpretation. Simply relating both CR production and UV (reprocessed to far-infrared) to star formation rates is apparently insufficient to explain the close correlation, and this has given rise to several different interpretations including hydrostatic regulation, without being very conclusive as yet (184; 185; 186).

3.9 Time- and space-dependent effects

CR propagation is usually modelled as a spatially smooth, temporally steady-state process. Because of the rapid diffusion and long containment time-scales in the Galaxy this is usually a sufficient approximation, but there are cases where it breaks down. The rapid energy loss of electrons above 100 GeV and the stochastic nature of their sources produces spatial and temporal variations. Supernovae are stochastic events and each SNR source of CR lasts only perhaps $10^4 - 10^5$ years, so that they leave their imprint on the distribution of electrons. This leads to large fluctuations in the CR electron density at high energies, so that the electron spectrum measured near the Sun may not be typical (113); a statistical calculation of this effect can be found in (145; 188) and for local SNR in (37). These effects are much smaller for nucleons since there are essentially no energy losses, but they can still be important (189); for the theory of CR fluctuations for a galaxy with random SNR events see (141) and Section 3.5. Such effects can influence the B/C ratio (111; 116) mainly through variations in the primary spectra. The local bubble can also have an effect on the energy-dependence of B/C (126). Dispersion in CR injection spectra from SNR may cause the locally observed spectrum to deviate from the average (147).

4 Summary Points list

Progress in CR research is rapid at the present time with the new generation of detectors for both direct and indirect measurements. But still it is hard to pin-down particular theories and even now the origin of the nucleonic component is not proven (34), although SNR are the leading candidates.

The main points we want to make are

- the importance of considering all relevant data, both direct (particles) and indirect (γ -ray, synchrotron) measurements
- increase in computing power has made many of the old approximations for interpreting CR data unnecessary
- new high-quality data will require detailed numerical models

5 Future Issues

We end by listing some of the open questions regarding CR propagation which might be answered with observations in the near future.

- the interpretation of the energy-dependence of the secondary/primary ratio, requiring accurate measurements at both, low and high energies
- the size of the propagation region – existence of an extended halo, requiring measurements of radioactive species over a broad energy range
- the relative roles of diffusion, convection and reacceleration
- the importance of local sources to the primary CR flux
- the origin of the GeV excess in γ -rays relative to the prediction based on locally observed CR
- the CR source distribution: is it like SNR or not?
- are positrons and antiprotons explained as secondaries from primary CR or is there a – perhaps exotic – excess?

In addition, on the theoretical side, we mention

- the relation of CR-dynamical models of the Galaxy to CR propagation theory

6 Related Resources

GALPROP website: <http://galprop.stanford.edu>,

GLAST website: <http://glast.stanford.edu>

7 Key terms, definitions and acronyms

Key terms/definitions:

Direct measurements: measurements on CR themselves with detectors in balloons and satellites. Indirect measurements: via electromagnetic radiation (γ -rays and synchrotron) emitted by CR interacting with interstellar matter and radiation fields. Primary CR: CR accelerated at sources (for example in SNR). Secondary CR: CR generated by spallation of primary CR on interstellar gas. p : particle momentum, R : particle magnetic rigidity = pc/Ze , β : velocity/speed-of-light, z_h : height of CR halo in direction perpendicular to Galactic plane

Acronyms:

ACE: Advanced Composition Explorer, B/C: cosmic-ray Boron-to-Carbon ratio, CMB: cosmic microwave background, CGRO: Compton Gamma Ray Observatory, CR: cosmic rays, EGRET: Energetic gamma-ray telescope, GALPROP: Galactic Propagation code, GLAST: Gamma-ray Large Area Telescope, H.E.S.S.: High Energy Stereoscopic System, ISRF: interstellar radiation field, PLD: path-length distribution, SNR: supernova remnant

8 Acknowledgements

I.V.M. acknowledges partial support from a NASA Astronomy and Physics Research and Analysis Program (APRA) grant.

References

1. Shapiro MM, Silberberg R. *Annu. Rev. Nuclear and Particle Sci.* 20:323 (1970)
2. Wentzel DG. *Annu. Rev. Astron. Astrophys.* 12:71 (1974)
3. Simpson JA. *Annu. Rev. Nuclear and Particle Sci.* 33:323 (1983)
4. Cesarsky CJ. *Annu. Rev. Astron. Astrophys.* 18:289 (1980)
5. Cox DP. *Annu. Rev. Astron. Astrophys.* 43:337 (2005)
6. Elmegreen BG, Scalo J. *Annu. Rev. Astron. Astrophys.* 42:211 (2004)
7. Scalo J, Elmegreen BG. *Annu. Rev. Astron. Astrophys.* 42:275 (2004)
8. Berezhinskii VS, Bulanov SV, Dogiel VA, Ptuskin VS. *Astrophysics of cosmic rays*, edited by VL Ginzburg. Amsterdam: North-Holland (1990)
9. Ginzburg VL, Syrovatskii SI. *The Origin of Cosmic Rays*. New York: Macmillan (1964)
10. Ginzburg VL, Ptuskin VS. *Rev. Mod. Phys.* 48:161 (1976)
11. Hillas AM. *Cosmic rays*, The Commonwealth and International Library, Selected Readings in Physics. Oxford: Pergamon Press (1972)
12. Gaisser TK. *Cosmic rays and particle physics*, 292 p. Cambridge and New York: Cambridge University Press, 1990
13. Stanev T. *High energy cosmic rays*, Praxis Books in Astrophysics and Astronomy. Chichester, UK: Springer (2004)
14. Schlickeiser R. *Cosmic ray astrophysics*, Astronomy and Astrophysics Library. Berlin: Springer (2002)
15. Diehl R, Parizot E, Kallenbach R, von Steiger R. in *The Astrophysics of Galactic Cosmic Rays*. Dordrecht: Kluwer (2002)
16. Nagano M, Watson AA. *Rev. Mod. Phys.* 72:689 (2000)
17. Cronin JW. *Nucl. Phys. B, Proc. Supp.* 138:465 (2005)
18. Hörandel JR. *astro-ph/0508014* (2005); *Journal of Physics: Conference Series* 47:41 (2006)
19. Engel R. *Nucl. Phys. B, Proc. Supp.* 151:437 (2006)
20. Stanev T. in *AIP Conf. Proc. 698: Intersections of Particle and Nuclear Physics*, p.357. New York: AIP (2004)
21. Berezhinsky V, Gazizov A, Grigorieva S. *Nucl. Phys. B, Proc. Supp.* 136:147 (2004)
22. Berezhinsky V, Gazizov A, Kachelrieß M. *astro-ph/0612247* (2006); *Phys. Rev. Lett.* 97:231101 (2006)
23. Hooper D, Sarkar S, Taylor AM. *astro-ph/0608085* (2006)
24. Hörandel JR. *Astropart. Phys.* 21:241 (2004)
25. Hillas AM. *astro-ph/0607109* (2006)
26. Gaisser TK. *astro-ph/0608553* (2006)
27. Kampert KH. *astro-ph/0611884* (2006)
28. Webber WR. *Astrophys. J.* 506:329 (1998)

29. Fatuzzo M, Adams FC, Melia F. *Astrophys. J.* 653:L49 (2006)
30. Hanasz M, Lesch H. *Astron. Astrophys.* 412:331 (2003)
31. Snodin AP, Brandenburg A, Mee AJ, Shukurov A. *MNRAS* 373:643 (2006)
32. Zirakashvili VN, Breitschwerdt D, Ptuskin VS, Völk HJ. *Astron. Astrophys.* 311:113 (1996)
33. Ptuskin VS, Völk HJ, Zirakashvili VN, Breitschwerdt D. *Astron. Astrophys.* 321:434 (1997)
34. Aharonian F, et al. *Astron. Astrophys.* 449:223 (2006)
35. Panov AD, et al. *astro-ph/0612377* (2006)
36. Derbina VA, et al. *Astrophys. J.* 628:L41 (2005)
37. Kobayashi T, Komori Y, Yoshida K, Nishimura J. *Astrophys. J.* 601:340 (2004)
38. Grimani C, et al. *Astron. Astrophys.* 392:287 (2002)
39. Moskalenko IV, Strong AW. *Astrophys. J.* 493:694 (1998)
40. Stephens SA. *Adv. Spa. Res.* 27:687 (2001)
41. Gast H, Olzem J, Schael S. *astro-ph/0605254* (2006)
42. Beatty JJ, et al. *Phys. Rev. Lett.* 93:241102 (2004)
43. Moskalenko IV, Strong AW, Ormes JF, Mashnik SG. *Adv. Spa. Res.* 35:156 (2005)
44. Bradt HL, Peters B. *Phys. Rev.* 80:943 (1950)
45. Garcia-Munoz M, Mason GM, Simpson JA. *Astrophys. J.* 201:L145 (1975)
46. Seo ES, Ptuskin VS. *Astrophys. J.* 431:705 (1994)
47. Webber WR. *Space Sci. Rev.* 86:239 (1998)
48. Wiedenbeck ME, et al. *Space Sci. Rev.* 99:15 (2001)
49. Connell JJ. *Space Sci. Rev.* 99:41 (2001)
50. Binns WR, et al. *Astrophys. J.* 634:351 (2005)
51. Kennel C, Engelmann F. *Phys. Fluids* 9:2377 (1966)
52. Casse F, Lemoine M, Pelletier G. *Phys. Rev. D.* 65:023002 (2002)
53. Jokipii JR. *Reviews of Geophysics and Space Physics* 9:27 (1971)
54. Toptygin IN. *Cosmic Rays in Interplanetary Magnetic Fields*. Dordrecht: Reidel (1985)
55. Goldreich P, Sridhar S. *Astrophys. J.* 438:763 (1995)
56. Yan H, Lazarian A. *Astrophys. J.* 614:757 (2004)
57. Breitschwerdt D, Komossa S. *Astrophys. Sp. Sci.* 272:3 (2000)
58. Breitschwerdt D, Völk HJ, McKenzie JF. *Astron. Astrophys.* 245:79 (1991)
59. Breitschwerdt D, McKenzie JF, Völk HJ. *Astron. Astrophys.* 269:54 (1993)
60. Jokipii JR. *Astrophys. J.* 208:900 (1976)
61. Owens AJ, Jokipii JR. *Astrophys. J.* 215:677 (1977)
62. Owens AJ, Jokipii JR. *Astrophys. J.* 215:685 (1977)
63. Jones FC. *Astrophys. J.* 222:1097 (1978)

64. Jones FC. *Astrophys. J.* 229:747 (1979)
65. Bloemen JBGM, Dogel' VA, Dorman VL, Ptuskin VS. *Astron. Astrophys.* 267:372 (1993)
66. Veilleux S, Cecil G, Bland-Hawthorn J. *Annu. Rev. Astron. Astrophys.* 43:769 (2005)
67. Strong AW, Moskalenko IV. *Astrophys. J.* 509:212 (1998)
68. Maurin D, Taillet R, Donato F. *Astron. Astrophys.* 394:1039 (2002)
69. Jones FC, Lukasiak A, Ptuskin V, Webber W. *Astrophys. J.* 547:264 (2001)
70. Breitschwerdt D, Dogiel VA, Völk HJ. *Astron. Astrophys.* 385:216 (2002)
71. Simon M, Heinrich W, Mathis KD. *Astrophys. J.* 300:32 (1986)
72. Letaw JR, Adams JHJr., Silberberg R, Tsao CH. *Astrophys. Sp. Sci.* 114:365 (1985)
73. Niebur SM, et al. in *AIP Conf. Proc. 528: Acceleration and Transport of Energetic Particles Observed in the Heliosphere*, ed. RA Mewaldt et al., p.406. New York: AIP (2000)
74. Jones FC, Lukasiak A, Ptuskin VS, Webber WR. *Adv. Spa. Res.* 27:737 (2001)
75. Ptuskin VS, et al. *Astrophys. J.* 642:902 (2006)
76. Wandel A, et al. *Astrophys. J.* 316:676 (1987)
77. Berezhko EG, et al. *Astron. Astrophys.* 410:189 (2003)
78. Moskalenko IV, Strong AW, Reimer O. in *ASSL Vol. 304: Cosmic Gamma-Ray Sources*, eds. KS Cheng and GE Romero, G. E., p.279. Dordrecht: Kluwer (2004)
79. Beck R. *Space Sci. Rev.* 99:243 (2001)
80. Han JL, et al. *Astrophys. J.* 642:868 (2006)
81. Strong AW, Moskalenko IV, Reimer O. *Astrophys. J.* 537:763 (2000)
82. Alvarez-Muñiz J, Engel R, Stanev T. *Astrophys. J.* 572:185 (2002)
83. Takami H, Yoshiguchi H, Sato K. *Astrophys. J.* 639:803 (2006)
84. Kachelriess M, Serpico PD, Teshima M. *astro-ph/0510444* (2005)
85. Moskalenko IV, Porter TA, Strong AW. *Astrophys. J.* 640:L155 (2006)
86. Frisch PC, Slavin JD. *astro-ph/0606743* (2006)
87. Frisch PC. *ASSL Vol. 338: Solar Journey: The Significance of our Galactic Environment for the Heliosphere and Earth*. Dordrecht: Springer (2006)
88. Moskalenko IV, Strong AW. *Astrophys. J.* 528:357 (2000)
89. Kamae T, et al. *Astrophys. J.* 647:692 (2006)
90. Kelner SR, Aharonian FA, Bugayov VV. *Phys. Rev. D.* 74:034018 (2006)
91. Müller D, et al. *Space Sci. Rev.* 99:353 (2001)
92. Mashnik SG, et al. *Adv. Spa. Res.* 34:1288 (2004)
93. Moskalenko IV, Strong AW, Mashnik SG. in *AIP Conf. Proc. 769: Int. Conf. on Nuclear Data for Science and Technology*, eds. RC Haight et al., p.1612. New York: AIP (2005)

94. de Nolfo GA, et al. *Adv. Spa. Res.* 38:1558 (2006)
95. Endt PM, van der Leun C. *Nucl. Phys. A* 310:1 (1978)
96. Martínez-Pinedo G, Vogel P. *Phys. Rev. Lett.* 81:281 (1998)
97. Wuosmaa AH, et al. *Phys. Rev. Lett.* 80:2085 (1998)
98. Strong AW, Moskalenko IV. *Adv. Spa. Res.* 27:717 (2001)
99. Davis LJr.. *Proc. 6th Int. Cosmic Ray Conf. (Moscow)* 3:220 (1960)
100. Protheroe RJ, Ormes JF, Comstock GM. *Astrophys. J.* 247:362 (1981)
101. Garcia-Munoz M, et al. *Astrophys. J. Suppl.* 64:269 (1987)
102. Ptuskin VS, Jones FC, Ormes JF. *Astrophys. J.* 465:972 (1996)
103. Stephens SA, Streitmatter RE. *Astrophys. J.* 505:266 (1998)
104. Davis AJ, et al. in *AIP Conf. Proc. 528: Acceleration and Transport of Energetic Particles Observed in the Heliosphere*, eds. RA Mewaldt et al., p.421. New York: AIP (2000)
105. Webber WR. *Astrophys. J.* 402:188 (1993)
106. Duvernois MA, Simpson JA, Thayer MR. *Astron. Astrophys.* 316:555 (1996)
107. Ptuskin VS, Soutoul A. *Astron. Astrophys.* 237:445 (1990)
108. Ptuskin VS, Soutoul A. *Astron. Astrophys.* 337:859 (1998)
109. Webber WR, Lee MA, Gupta M. *Astrophys. J.* 390:96 (1992)
110. Maurin D, Donato F, Taillet R, Salati P. *Astrophys. J.* 555:585 (2001)
111. Taillet R, et al. *Astrophys. J.* 609:173 (2004)
112. Higdon JC, Lingenfelter RE. *Astrophys. J.* 582:330 (2003)
113. Strong AW, Moskalenko IV, Reimer O. *Astrophys. J.* 613:962 (2004)
114. Shibata T, Hareyama M, Nakazawa M, Saito C. *Astrophys. J.* 612:238 (2004)
115. Shibata T, Hareyama M, Nakazawa M, Saito C. *Astrophys. J.* 642:882 (2006)
116. Büsching I, et al. *Astrophys. J.* 619:314 (2005)
117. Moskalenko IV, Strong AW, Ormes JF, Potgieter MS. *Astrophys. J.* 565:280 (2002)
118. Wallace JM. *Astrophys. J.* 245:753 (1981)
119. Hanasz M, Lesch H. *Astrophys. J.* 543:235 (2000)
120. Giacalone J, Jokipii JR. *Astrophys. J.* 520:204 (1999)
121. Hanasz M, Kowal G, Otmianowska-Mazur K, Lesch H. *Astrophys. J.* 605:L33 (2004)
122. Moskalenko IV, Mashnik SG. *Proc. 28th Int. Cosmic Ray Conf. (Tsukuba)* 4:1969 (2003)
123. Webber WR, McDonald FB, Lukasiak A. *Astrophys. J.* 599:582 (2003)
124. Shalchi A, Bieber JW, Matthaeus WH, Qin G. *Astrophys. J.* 616:617 (2004)
125. Shalchi A, Schlickeiser R. *Astrophys. J.* 626:L97 (2005)
126. Moskalenko IV, Strong AW, Mashnik SG, Ormes JF. *Astrophys. J.* 586:1050 (2003)
127. Donato F, Maurin D, Taillet R. *Astron. Astrophys.* 381:539 (2002)

128. Moskalenko IV, Mashnik SG, Strong AW. *Proc. 27th Int. Cosmic Ray Conf. (Hamburg)* 5:1836 (2001)
129. Hams T, et al. *Astrophys. J.* 611:892 (2004)
130. Streitmatter RE, Stephens SA. *Adv. Spa. Res.* 27:743 (2001)
131. Ptuskin VS, Soutoul A. *Space Sci. Rev.* 86:225 (1998)
132. Yanasak NE, et al. *Astrophys. J.* 563:768 (2001)
133. Mewaldt RA, et al. *Space Sci. Rev.* 99:27 (2001)
134. Mueller HR, Frisch PC, Florinski V, Zank GP. *astro-ph/0607600* (2006)
135. Wiedenbeck ME, et al. in *AIP Conf. Proc. 528: Acceleration and Transport of Energetic Particles Observed in the Heliosphere*, p.363. New York: AIP (2000)
136. de Nolfo GA, et al.. *Proc. 29th Int. Cosmic Ray Conf. (Pune)* 3:61 (2005)
137. Niebur SM, et al. *Proc. 27th Int. Cosmic Ray Conf. (Hamburg)* 5:1675 (2001)
138. Amenomori M, et al. *Astrophys. J.* 626:L29 (2005)
139. Tada J, et al. *Nucl. Phys. B, Proc. Supp.* 151:485 (2006)
140. Guillian G. *Proc. 29th Int. Cosmic Ray Conf. (Pune)* 6:85 (2005)
141. Ptuskin VS, Jones FC, Seo ES, Sina R. *Adv. Spa. Res.* 37:1909 (2006)
142. Ambrosio M, et al. *Phys. Rev. D.* 67:042002 (2003)
143. Moskalenko IV, Strong AW. in *AIP Conf. Proc. 801: Astrophysical Sources of High Energy Particles and Radiation*, eds. T Bulik et al., p.57. New York: AIP (2005)
144. Strong AW, et al. *Astron. Astrophys.* 422:L47 (2004)
145. Pohl M, Esposito JA. *Astrophys. J.* 507:327 (1998)
146. Moskalenko IV, Strong AW, Reimer O. *Astron. Astrophys.* 338:L75 (1998)
147. Büsching I, Pohl M, Schlickeiser R. *Astron. Astrophys.* 377:1056 (2001)
148. de Boer W, et al. *Astron. Astrophys.* 444:51 (2005)
149. Bergström L, Edsjö J, Gustafsson M, Salati P. *JCAP* 5:6 (2006)
150. Moskalenko IV, et al. *astro-ph/0609768* (2006)
151. Strong AW, et al. *Astron. Astrophys.* 444:495 (2005)
152. Sasaki M, Breitschwerdt D, Supper R. *Astrophys. Sp. Sci.* 289:283 (2004)
153. Golden RL, et al. *Phys. Rev. Lett.* 43:1196 (1979)
154. Bogomolov EA, et al. *Proc. 19th Int. Cosmic Ray Conf. (La Jolla)* 2:362 (1985)
155. Mitchell JW, et al. *Phys. Rev. Lett.* 76:3057 (1996)
156. Hof M, et al. *Astrophys. J.* 467:L33 (1996)
157. Grimani C, et al. *Astron. Astrophys.* 392:287 (2002)
158. Orito S, et al. *Phys. Rev. Lett.* 84:1078 (2000)
159. Bergström D, et al. *Astrophys. J.* 534:L177 (2000)
160. Sanuki T, et al. *Astrophys. J.* 545:1135 (2000)
161. Maeno T, et al. *Astropart. Phys.* 16:121 (2001)

162. Asaoka Y, et al. *Phys. Rev. Lett.* 88:051101 (2002)
163. Moskalenko IV, Strong AW, Mashnik SG, Ormes JF. *Proc. 28th Int. Cosmic Ray Conf. (Tsukuba)* 4:1921 (2003)
164. Picozza P, et al. *astro-ph/0608697* (2006)
165. de Shong JA, Hildebrand RH, Meyer P. *Phys. Rev. Lett.* 12:3 (1964)
166. Protheroe RJ. *Astrophys. J.* 254:391 (1982)
167. Coutu S, et al. *Astropart. Phys.* 11:429 (1999)
168. Chi X, Cheng KS, Young ECM. *Astrophys. J.* 459:L83 (1996)
169. Baltz EA, Edsjö J. *Phys. Rev. D.* 59:023511 (1999)
170. AMS Collaboration, et al. *Phys. Rep.* 366:331 (2002)
171. Boezio M, et al. *Astrophys. J.* 532:653 (2000)
172. DuVernois MA, et al. *Astrophys. J.* 559:296 (2001)
173. Ellison DC. *Space Sci. Rev.* 99:305 (2001)
174. Allen G. *Proc. 26th Int. Cosmic Ray Conf. (Salt Lake City)* 3:480 (1999)
175. Beuermann K, Kanbach G, Berkhuijsen EM. *Astron. Astrophys.* 153:17 (1985)
176. Broadbent A, Haslam TCG, Osborne LJ. *Proc. 21st Int. Cosmic Ray Conf. (Adelaide)* 3:229 (1990)
177. Beck R. in *The Magnetized Plasma in Galaxy Evolution*, eds. KT Chyzy et al., p.193. Kraków: Jagiellonian University (2005)
178. Beck R. *astro-ph/0603531* (2006)
179. Allen RJ, Sancisi R, Baldwin JE. *Astron. Astrophys.* 62:397 (1978)
180. Heald GH, Rand RJ, Benjamin RA, Bershadsky MA. *Astrophys. J.* 647:1018 (2006)
181. Dumke M, Krause M. in *LNP Vol. 506: Proc. IAU Colloq. 166, The Local Bubble and Beyond*, eds. D Breitschwerdt et al., p.555. Berlin: Springer (1998)
182. Heesen V, Krause M, Beck R, Dettmar RJ. in *The Magnetized Plasma in Galaxy Evolution*, eds. KT Chyzy et al., p.156. Kraków: Jagiellonian University (2005)
183. Beck R, Krause M. *Astronomische Nachrichten* 326:414 (2005)
184. Niklas S, Beck R. *Astron. Astrophys.* 320:54 (1997)
185. Murgia M, et al. *Astron. Astrophys.* 437:389 (2005)
186. Paladino R, et al. *Astron. Astrophys.* 456:847 (2006)
187. Völk HJ. *Astron. Astrophys.* 218:67 (1989)
188. Strong AW, Moskalenko IV. *Proc. 27th Int. Cosmic Ray Conf. (Hamburg)* 5:1964 (2001)
189. Erlykin AD, Wolfendale AW. *J. Phys. G: Nucl. Part. Phys.* 28:359 (2002)

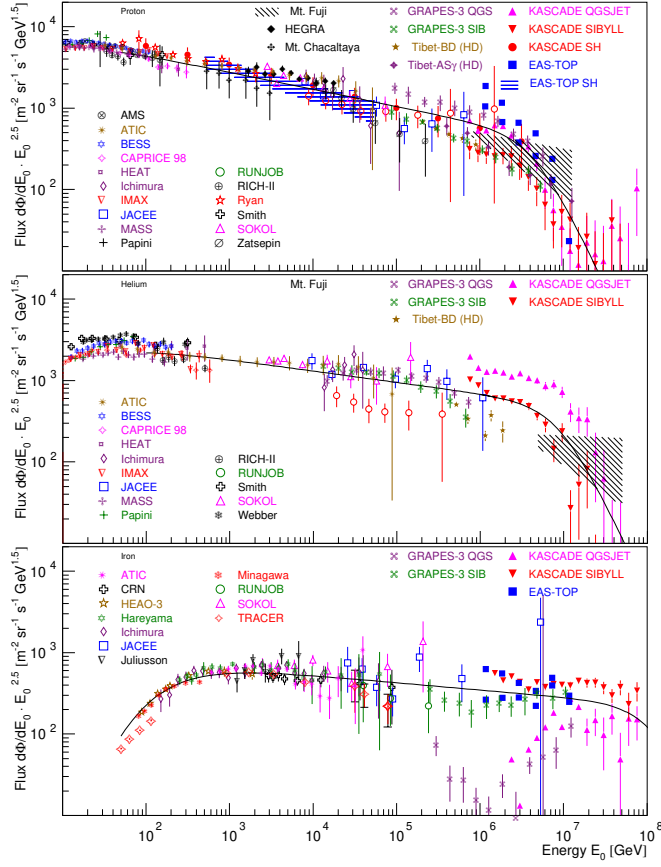


Figure 1: Compilation of spectral data $10^{10} - 10^{17}$ eV for p, He, Fe, combining balloon, satellite and ground-based measurements. From (18) and G. Hörandel, private communication.

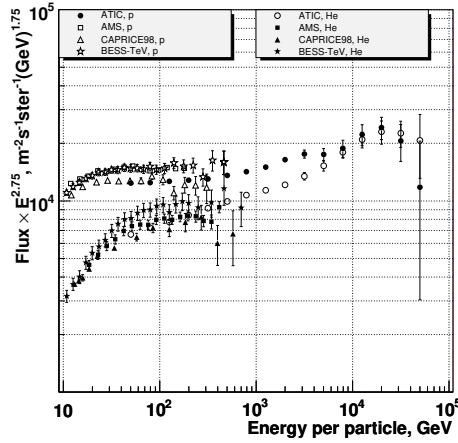


Figure 2: Preliminary spectra of p, He from ATIC-2, compared with AMS01, BESS-TeV and CAPRICE98. Plot from ATIC collaboration (35). The ATIC-2 data indicate a slightly harder spectrum for He above 1 TeV.

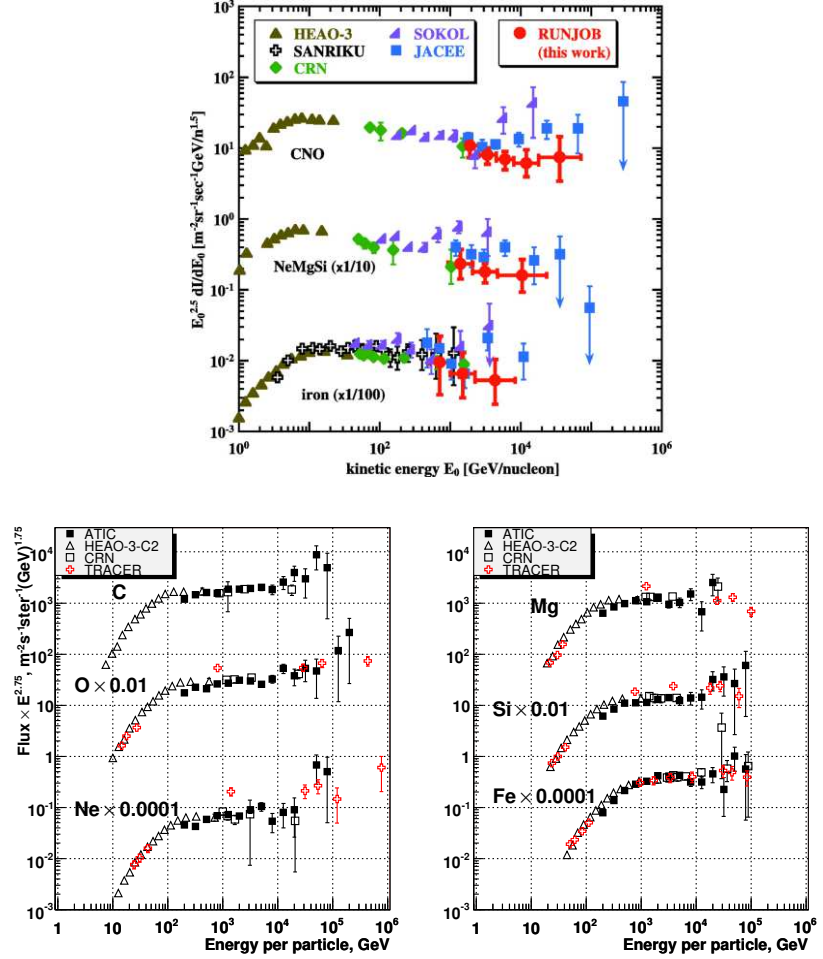


Figure 3: Compilation of spectral data for element groups CNO, NeMgSi, Fe (36) from HEAO-3, SANRIKU, CRN, SOKOL, JACEE and RUNJOB (upper) and of separate even-Z elements from preliminary ATIC-2, HEAO-3, CRN and TRACER (lower). Plot from ATIC collaboration (35). The ATIC-2 data suggest a hardening above 10 TeV.

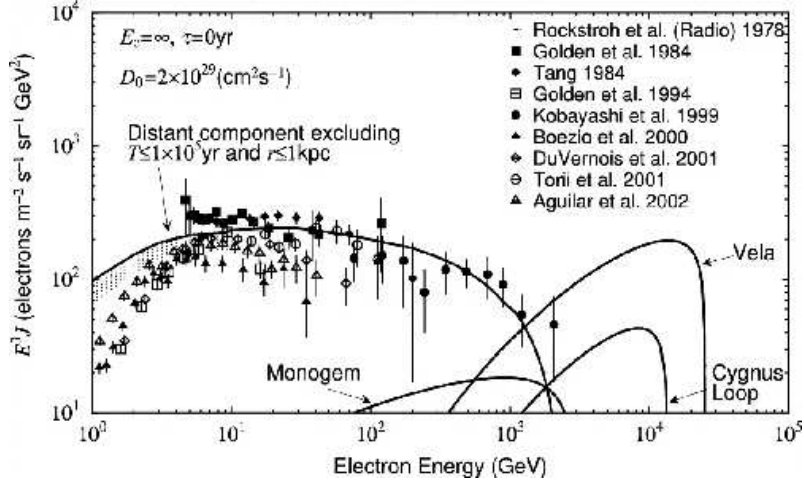


Figure 4: Measurements of the electron spectrum, including AMS01, CAPRICE94, HEAT and SANRIKU, compared with possible contributions of distant sources and local supernova remnants, from (37).

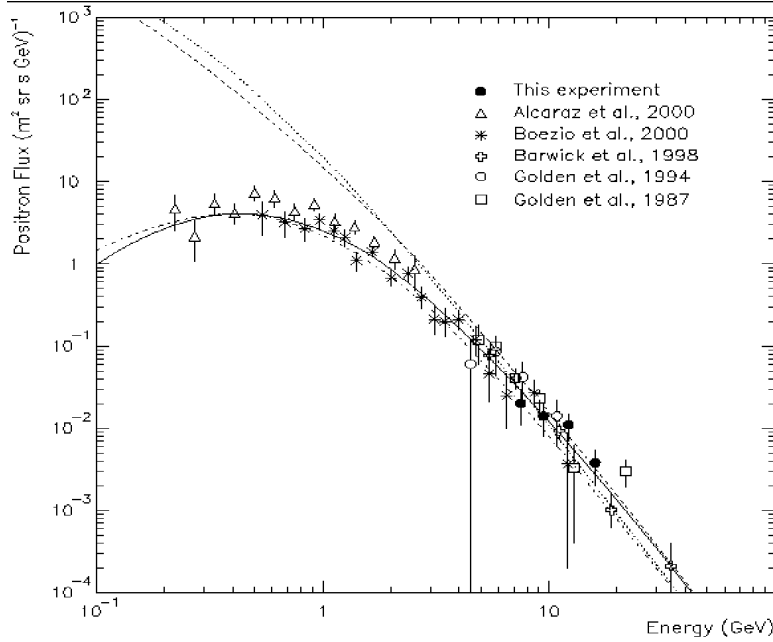


Figure 5: Measurements of the positron spectrum, including data from MASS91, AMS01, CAPRICE94 and HEAT, from (38). Propagation calculations for interstellar (upper curves) and modulated (lower curves) are shown. Dotted, dot-dashed: GALPROP (39); dashed, solid: (40).

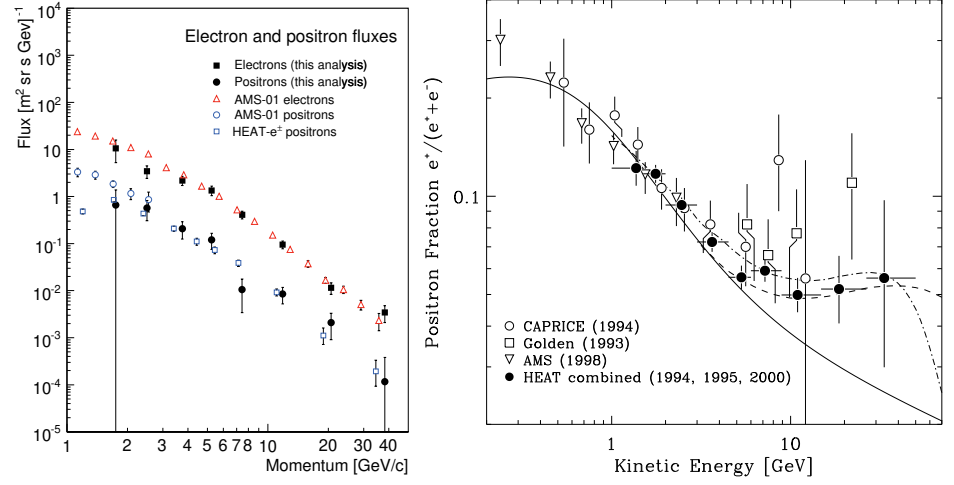


Figure 6: Left: Measurements of the electron and positron spectrum by AMS01 and HEAT, from (41). Right: $e^+/(e^+ + e^-)$ ratio including HEAT and AMS01 (42). For the ratio a propagation calculation (39) is shown by the solid line, and possible contributions from pulsars (dashed) and dark matter annihilations (dash-dot).

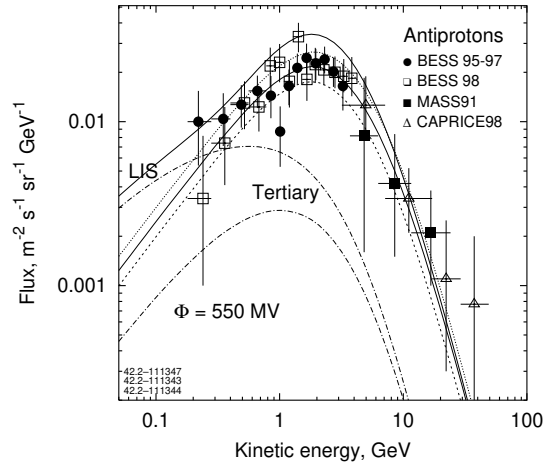


Figure 7: Measurements of the antiproton spectrum from MASS91, CAPRICE98 and BESS, compared to a propagation calculation, from (43). The dashed and dotted lines illustrate the sensitivity of the calculated (modulated) antiproton flux to the normalization of the diffusion coefficient. LIS marks the local interstellar spectrum.

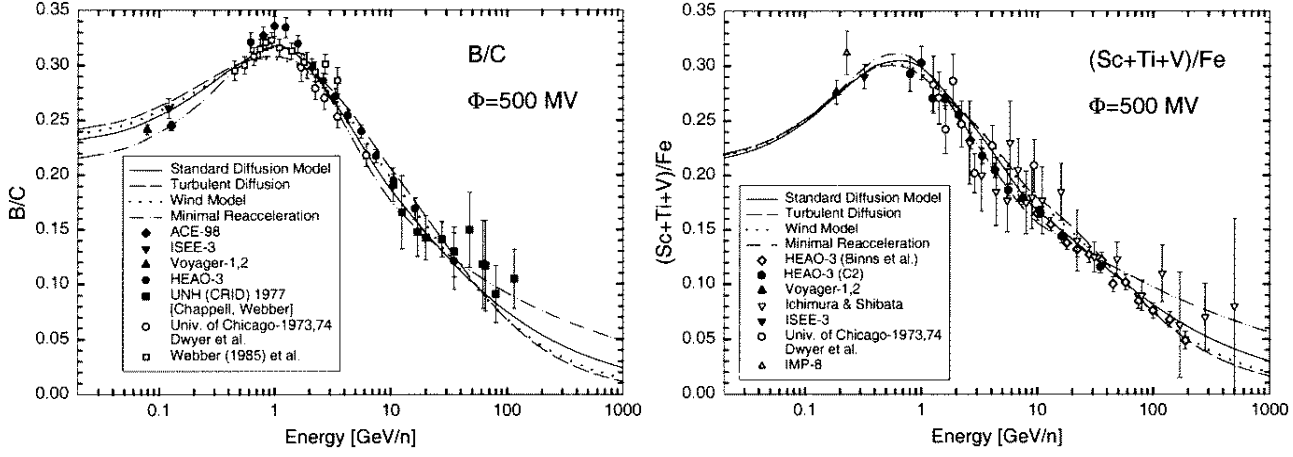


Figure 8: B/C and sub-Fe/Fe data compilation compared to four models treated by the modified weighted-slab technique, from (69).

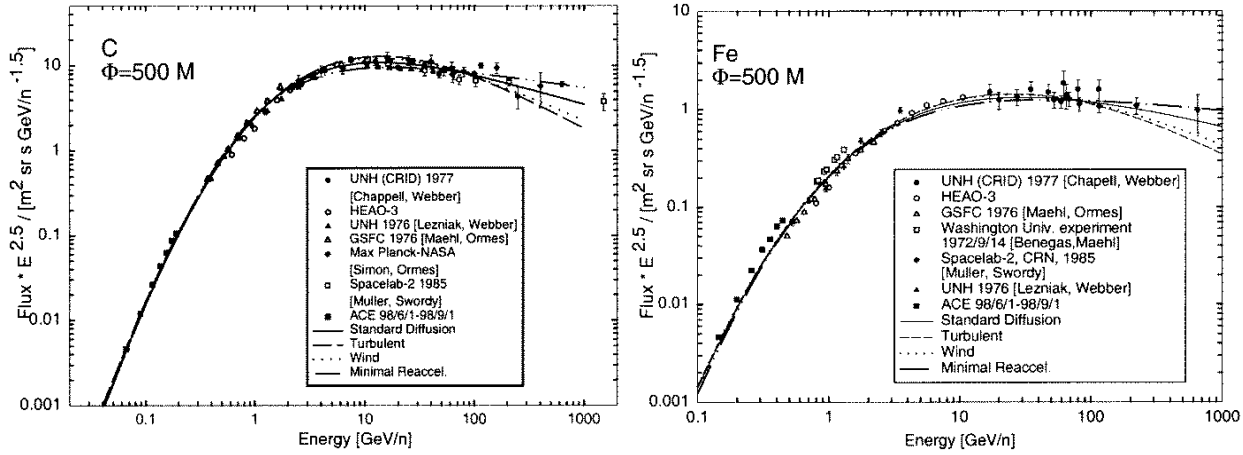


Figure 9: Data compilation for spectra of C and Fe compared to four models treated by the modified weighted-slab technique, from (69).

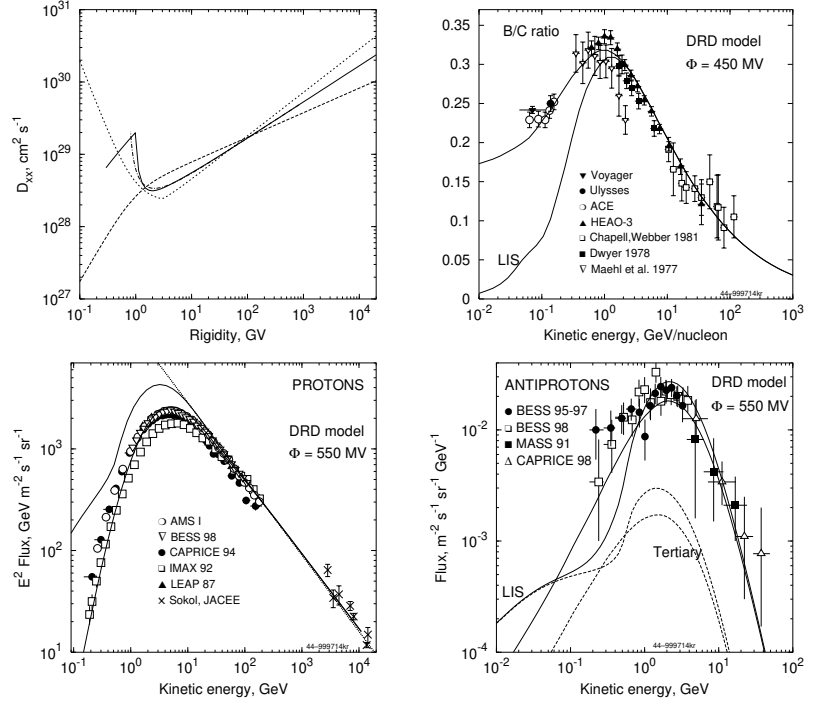


Figure 10: Upper left: diffusion coefficient in different models (75): plain diffusion (dots), Kolmogorov reacceleration (dashes), and Kraichnan-type reacceleration with wave-damping (solid). Upper right: B/C, lower left: protons, lower right: antiprotons, in the wave-damping model (75). LIS marks the local interstellar spectrum.

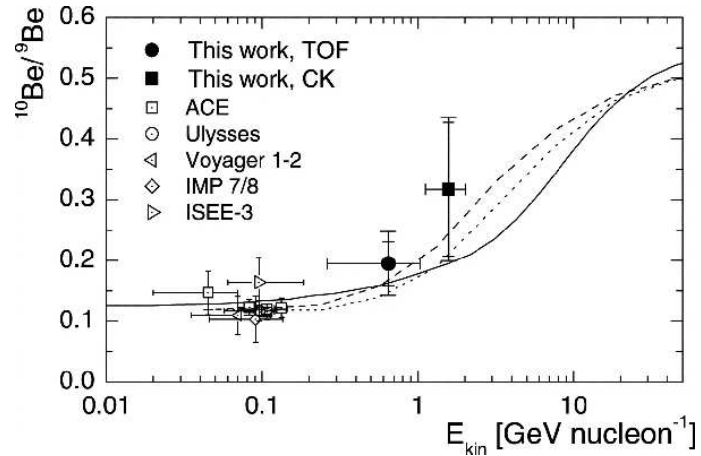


Figure 11: Data on energy-dependence of $^{10}\text{Be}/^9\text{Be}$ including ACE, Ulysses, Voyager, IMP, ISEE-3 and ISOMAX data, from (129). The solid line is a diffusive halo model with 4 kpc scale height using GALPROP (98) the other lines are leaky-box models (130).

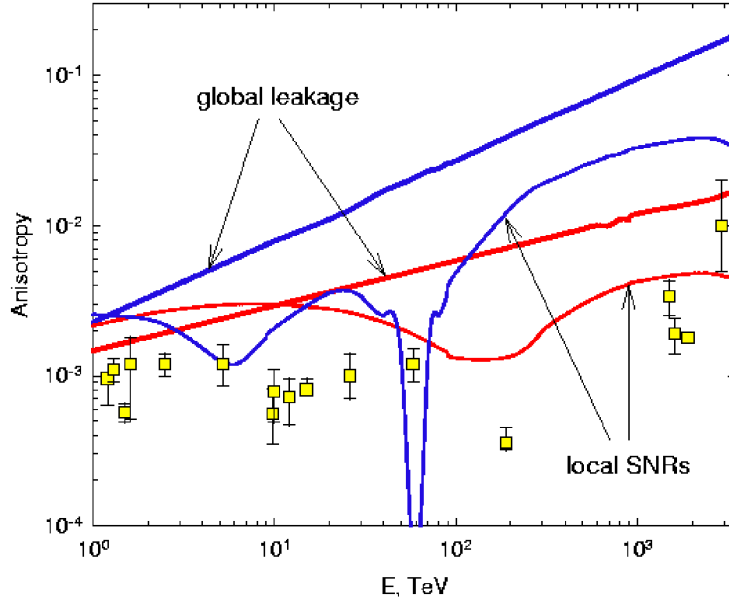


Figure 12: The anisotropy of cosmic rays in the reacceleration (red curves) and the plain diffusion (blue curves) models. Separately shown are the effects of the global leakage from the Galaxy (thick lines), and the contribution from local SNR (thin lines). The collection of data on cosmic ray anisotropy (yellow squares) are taken from (142) where the references to individual experiments can be found.

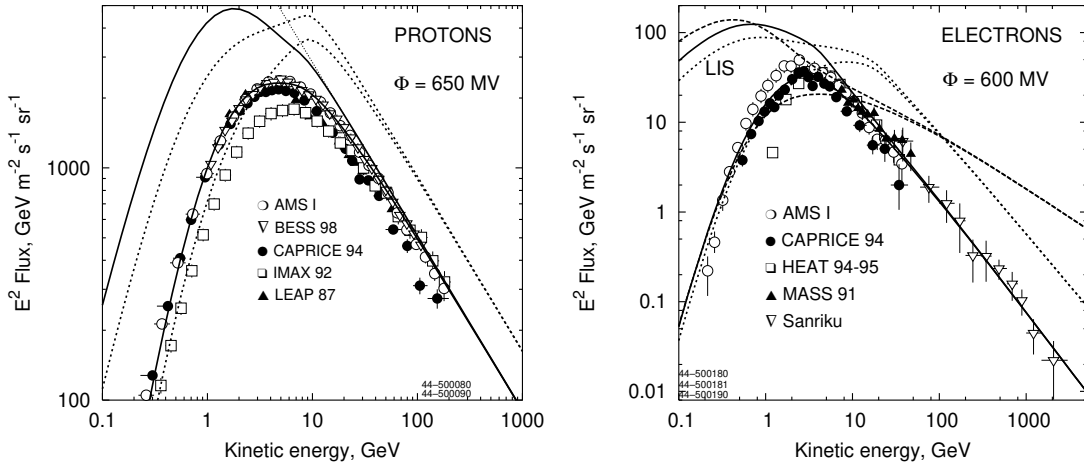


Figure 13: Directly-observed (solid), and modified (dots) proton and electron spectra. The modified spectra are deduced from fits to antiproton and γ -ray data (113). LIS marks local interstellar spectra. Data shown are from AMS01, BESS, CAPRICE94, IMAX, LEAP, HEAT, MASS91, SANRIKU.

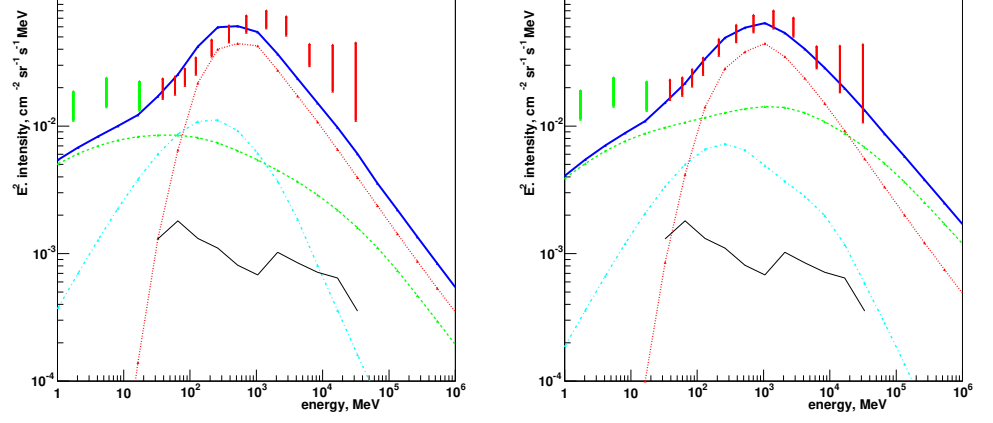


Figure 14: γ -ray spectrum of inner Galaxy ($330^\circ < l < 30^\circ$, $|b| < 5^\circ$) for model based on the directly-observed CR spectra and modified spectra shown in Fig. 13. Red bars: EGRET data, including points above 10 GeV, see (151). Green bars: COMPTEL. Light blue line: bremsstrahlung, green line: inverse Compton scattering, red line: π^0 -decay, black line: extragalactic background, dark blue line: total. This is an update of the spectra shown in (113).

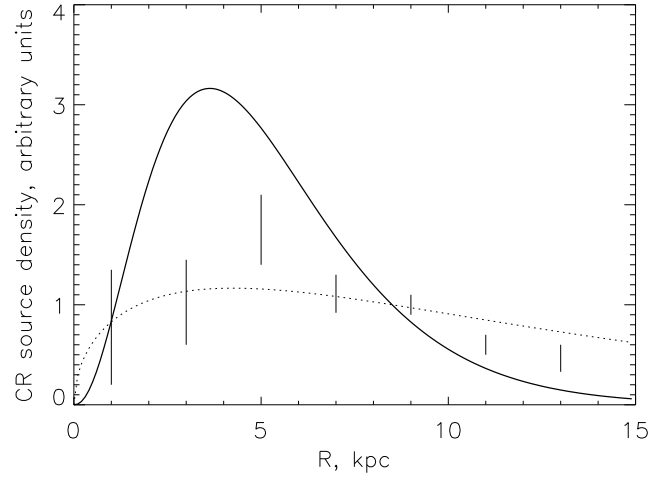


Figure 15: Possible CR source distributions as function of Galactocentric radius R : pulsars (solid line), SNR (vertical bars), from γ -rays assuming constant H_2 -to-CO relation (dotted line) (144).

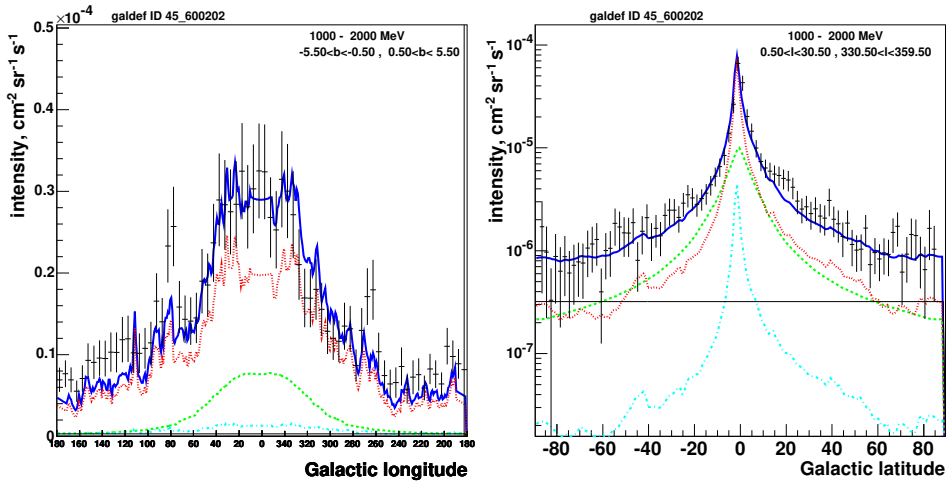


Figure 16: γ -ray longitude and latitude profiles, for model with pulsar source distribution and X_{co} varying with radius (144). Light blue line: bremsstrahlung, green line: inverse Compton scattering, red line: π^0 -decay, black line: extragalactic background, dark blue line: total.